CHEMICAL SYNTHESIS OF HYDROXYAPATITE FROM WASTE NATURAL BIOLOGICAL SOURCES AND THEIR COMPARATIVE ANALYSIS.

Project Report

Submitted in partial fulfilment of the requirements for the degree of

Master of Technology Biotechnology

Submitted by

T Rashmi

11203499

Under the guidance of

Dr.Anjuvan Singh

Associate Professor

SCHOOL OF BIOENGINEERING AND BIOSCIENCES LOVELY

PROFESSIONAL UNIVERSITY PHAGWARA, PUNJAB-144411

CERTIFICATE

This is to certify that **T Rashmi (11203499)** have completed the project entitled "**chemical synthesis of hydroxyapatite from waste natural biological sources and their comparative analysis**" under my guidance and supervision. To the best of my knowledge, the present work is the result of their original investigation and study.

No part of the report has ever been submitted for any other degree at any University. The report is fit for submission and the partial fulfillment of the conditions for the award of M. Tech in biotechnology.

Date: Supervisor Signature:

ACKNOWLEDGEMENTS

First of all I thank **GOD ALMIGHTY** for showering his grace on us.

It is a privilege to express my gratitude and respect to all those who guided and inspired me in the partial completion of this project. I sincerely express my gratitude to our beloved Head of School, **Dr. Neeta Raj Sharma, Ph.D.,** School of Bioengineering and Biosciences.

I express my grateful thanks to **Mr. Himanshu Singh.,** Head of the Department, Department of Biotechnology, for his valuable help during the course of the present study.

I am extending my gratitude to **Dr. Anjuvan Singh.,** Associate Professor and Internal guide who kindly permitted me to do this project work and for his constant encouragement and guidance provided to carry out this study in this institution.

I also wish to express my thanks to all the members of Lovely professional University for their kind assistance throughout my work.

I also thank my staff members, parents, friends and who supported me till the end of project.

DECLARATION STATEMENT

We hereby declare that the project entitled "*chemical synthesis of hydroxyapatite from waste natural biological sources and their comparative analysis*" is an authentic record of our own work carried out at School of Bioengineering and Biosciences, Lovely Professional University, Phagwara, for the partial fulfilment of the award of Master of Technology in Biotechnology under the guidance of ***Dr. Anjuvan Singh.***

This work is our original work and has not been submitted for any degree/diploma in this or any other University. The information furnished in this report is genuine to the best of my knowledge and belief.

Place: T.Rashmi (11203499)
Date:

CONTENTS

ABSTRACT

The hydroxyapatite resembles that of natural bone. Recent study reveals that the hydroxyapatite can be substituted for fractured bones. The isolation of hydroxyapatite from rich calcium sources like egg shells, oyster shells, crab shells gives a cue to analyze their properties (resembling natural bone). The comparative analysis study is done to prove its importance and its usage in the real life.

LIST OF FIGURES

LIST OF ABBREVIATIONS

HA	Hydroxyapatite
HAP	Hydroxyapatite powder
SEM	Scanning electron microscopy
TEM	Transmission electron microscopy
XRD	X – Ray Diffraction
FTIR	Fourier Transform Infrared Spectrophotometry
TCP	TriCalcium Phosphate
TTCP	TetraCalcium Phosphate
DCPD	DiCalcium Phosphate Dihydrate
DCPA	DiCalcium Phosphate Anhydrate
ACP	Amorphous Calcium Phosphate

LIST OF SYMBOLS

%	-----	Percentage
µl	-----	Micro liter
×	-----	Multiplication
/	-----	Division
^	-----	Power of
C	-----	Degree Celsius
nm	-----	Nanometer
ml	-----	Milliliter

CHAPTER – 1
INTRODUCTION

INTRODUCTION

Hydroxyapatite ($Ca1_0(PO_4)_6(OH)_2$, HA) is the hydroxyl end member of the complex apatite group. The OH^- ion can be substituted by carbonate, chloride or fluoride, producing chlorapatite or fluorapatite. It crystallizes in the hexagonal crystal system. Pure hydroxylapatite powder is white in colour. Universally occurring apatites can also have brown, yellow, or green colorations, tantamount to the discolorations of dental fluorosis.

Up to 70% by weight and 50% by volume of human bone is a changed form of hydroxylapatite (known as bone mineral) [Junqueir *et al.*,2003].Dentin and dental element care composed of main mineral that is carbonated calcium-deficient hydroxylapatite. Small calcification of hydroxyapatite crystals (found in the pineal gland) called as 'brain sand' or corpora arenacea.

It is the important mineral composition to human bones and teeth, the major withdraw in arrangement being a changeable Ca/P mol ratio is 1.67. Being HA a biocompatible, non-toxic, non-immunogenic agent, non-inflammatory, but also bioactive [Fathi M.H *et al.*,2008]. The host bone is directly bonded by HA as artificial bones or teeth. It is majorly used in orthopedic applications [Zhang X,2007].

Hydroxyapatite can be synthesized through several methods such as wet chemical deposition, biomimetic deposition, sol-gel path (wet-chemical precipitation) or electrodeposition. [Ferraz *et al.*,2004]Yagai and Aoki stated that the hydroxyapatite nanocrystal suspension can be done via wet chemical precipitation reaction following the reaction equation below: [Bouyer *et al.*,2000].

$$10\ Ca(OH)_2 + 6\ H_3PO_4 \rightarrow Ca_{10}(PO_4)_6(OH)_2 + 18\ H_2O$$

Many research have shown that hydroxyapatite synthesis through wet-chemical path can be improved by power ultrasound. Nano structured hydroxyapatite of great quality can be produced by a successful technique which is ultrasonically assisted synthesis of HA. The ultrasonic path permits to produce nano-crystalline hydroxyapatite and also modified particles, example: core-shell, nanospheres and many composites.

The aim of the experiment is to synthesize hydroxyapatite from common and cheap sources such as oyster shell, egg shell and crab shell. The calcium carbonate is converted into calcium hydroxide at high temperature i.e. 800^oC. Then the calcium hydroxide is treated with several chemicals such as ammonia solution and orthophosphoric acid to synthesis HA.

Hydroxylapatite is a constituent in teeth and bones in the human body. Hence, it is generally used as a filler to substitute excised bone or as an encrustation to endorse bone ingrowth into prosthetic implants. Eventhough several other phases exist with similar or identical chemical makeup, the body reacts to them very distinctly. Coral skeletons can be converted into hydroxylapatite by steep temperatures; their penetrable structure permits comparatively fast ingrowth at the rate of original mechanical strength.

Regardless of enticing biological features, hydroxylapatite, and materials based eventually, have some flaws, such as less bioresorption rate in vivo, ailing triggering result on the development of newly bone tissues, low crack resistance and limited fatigue endurance in the corporeal surrounding. The function of changed hydroxylapatite opens up the fortuity for the development of synthetic or unreal osseous mater for implants and a wide range of drugs for medicating several lesions of bone, delicate and muculent tissues of the personal. A reassuring process of alteration is the installation of fluorine or silicon into the elementary conformation with the production of fluorine- or silicon-substituted hydroxylapatite[Bogdanova *et al.*,2014].The addition of fluorine maximizes the withstand to biodegradation [Cheng *et al.*,2004] and ameliorates the adsorption of proteins and adherence of the encrustation to the metal substrate [Zhang *et al.*,2006].

.

CHAPTER – 2
TERMINOLOGY

TERMINOLOGY

FTIR

FT-IR (Fourier Transform InfraRed) is a technique of obtaining infrared spectra by basically amalgating an interferogram of a sample signal using an interferometer, and then doing a Fourier Transform (FT) on the interferogram to get the spectrum.

SEM :

SEM is Scanning Electron Microscopy. It is a kind of electron magnifying lens which helps in making pictures of an analyte by the particular component of filtering of electrons in a focussed shaft

XRD :

X-beam powder diffraction (XRD) is a quick analytical strategy essentially utilized for stage distinguishing proof of a crystalline material and can give data on unit cell measurements.

STRETCHING :

Stretching is a change in the length of a bond, such as C-H or C-C.

BENDING :

Bending is a change in the angle between two bonds, such as the HCH angle in a methylene group.

CHAPTER – 3
REVIEW OF LITERATURE

REVIEW OF LITERATURE

3.1 General Literature on Hydroxyapatite

Naturally occuring hydroxyapatite sources like scaffoldings of marine organisms(coral, sea urchins, oyster shells, conch and clam shells,etc.), fish bone and egg shells are worthless after the exercise of their fillings and are generally deliberated as contamination to the environment because they support bacterial replication[Rhind SM,2009].Nevertheless, this waste is obtainable in all sort of advanced and underdeveloped societies in large amount from food treating plants, egg baking and breeding farms. They have been earlier operated as calcium source for generating calcium phosphates ceramics to be practiced on tissue engineering and biomedical as bone alternate.

Through different available calcium phosphate ceramics, Hydroxylapatite (HA) having the common formula Ca10(PO4)6(OH)2 is recognized artificial substance operated for their placement for human bone on account of its outstanding biocompatibility in human body. Above pH 4.3 it shows outstanding phase stability and as the human blood have the pH around7.3,HA is acceptable substitute matter for functions including blood contact.

Prime factor which separates hydroxyapatite from different calcium phosphate ceramics (i.e. Ca3(PO4)2 that is TCP) is the greater in vivo stability of the former substance with reference to TCP. Hydroxyapatite is also an vital constituent of osseous matter and have compositional and anatomical likeness to that of human bone with ions correspondence to that formed in physiological environment.All these above mentioned properties of hydroxyapatite makes it a better biocompatible substance with an revised bone connecting capability along the bone – implant admix. The bone connecting takes place through the production of a slender apatite coating as a outcome of the reaction ‘tween HA and body fluid. It has also been observed that the crystal structure,degree of crystallinity, is highly regulated via pH. Hence, several research have been carried out to comprehend the result of crystal structure on the encircling behaviour of the apatite in body surroundings.

The location of $(Ca)^{2+}$, $(PO_4)^{3-}$ and $(OH)^-$ ions in the HA the unit cell is shown below:

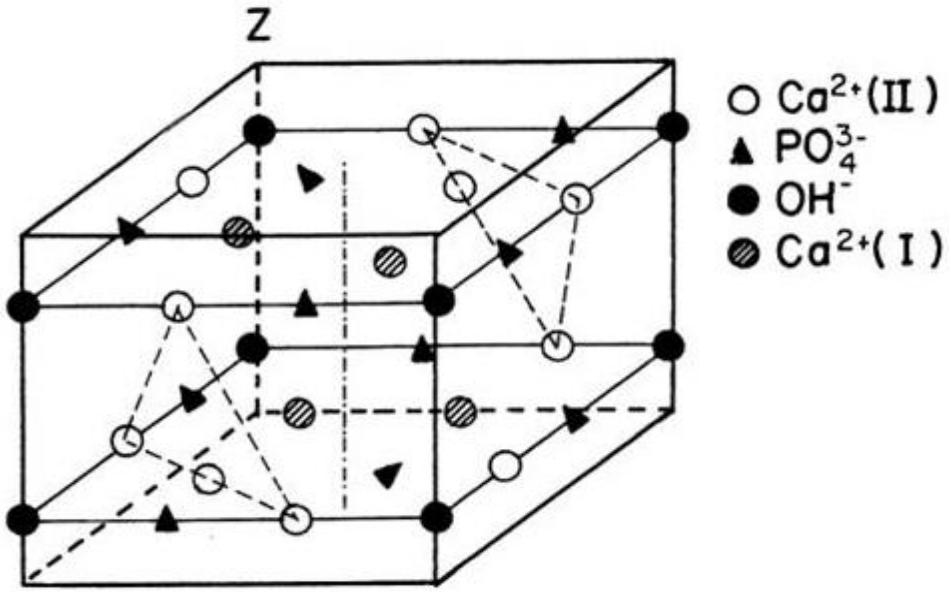

Fig. 2.1 Unit Cell structure of hydroxyapatite (HA)

The unit cell consists of ten Ca2+ ions. Out of these, six Ca2+ ions lie totally inside the unit cell at Ca(II) location each creating a triangular group of three Ca2+ ions at z = 0.25 and z = 0.75 consequently. The Ca2+ ions encloses the (OH)- groups at the edges of the unit cell at z = 0.25 and z = 0.75. Eight other Ca2+ ions lie at the verge of Ca(I) location and being shared by neighboring unit cells, so that the distribution for each unit cell is four. Similarly the eight (OH)- ions lying at the corner of every unit cell is being shared by neighboring unit cell to produce a residual of two to each unit cell. At last, out of the ten (PO4)3- group two lies totally inside the unit cell and eight at the verge with an total contributing of six to each unit cell.In the initial seventies, a number of research stated that Hydroxyapatite occured in two distinct crystalline forms i.e. monoclinic and hexagonal. Dense unnatural Hydroxyapatite generally consists of a hexagonal structure (S.G. P63/m, 2 formula units per cell) with cell dimensions a=b=9.42 Å and c=6.8 8Å (six- fold symmetry axis with a three-fold helix and a micro plane). Ca/P molar ratio for Hydroxyapatite is 1.67 and weight ratio of Ca/P is 2.151.The theoretical density of Hydroxyapatite is 3.153 $gm.cm^{-1}$.Hydroxyapatite can be produced by a number of ways solid state reactions between CaO and P2O5 as well as by other chemical path such as sol gel, mechano-chemical synthesis, microwave irradiation method etc. Eventhough solid state reaction

path is the simplest to comprehend but it is hard to control the initial purity of raw materials, and the path usually produces inhomogeneous non stoichiometric hydroxyapatite which want steep temperature for hydroxyapatite production. In the other hand, chemical synthesis path yield phase genuine hydroxyapatite at a much lesser processing temperature. hence, it is crucial to comprehend and confer the result of other processing methods on the phase stability of hydroxyapatite, its crystallinity, eventual Ca/P ratio in hydroxyapatite, stoichiometry and the ultimate mechanical characteristic of HA. Hence, this portion makes a detailed study on such aspects of powder processing.

3.2 Processing of HA

3.2.1 Synthesis of HA by Wet Precipitation Route

Guzman et.al incorporated stoichiometric HAP by two distinct ways: wet precipitation route and sol gel method. In the first, two distinct ways of wet precipitation paths were used. The former precipitation path used Ca(OH)2 and H3PO4 as predecessor and the later precipitation path used Ca(NO3)2 and (NH4)2HPO4 as the beginning material. The precipitates from the precipitation path were calcined at 800^{o}C and constantly maintained. Besides, sintering additives (~ 2.5 wt%) did not effect the phases of pure hydroxyapatite.

Jillavenkatesa et.al incorporated HA by sol-gel path utilizing calcium acetate and triethyl phosphate as calcium and phosphate point source. Different organic alcohols were also supplemented to analyse their result on the response. It was noticed that gradual amount of hydrolysis of phosphate could be stimulated by using organic alcohols. However, it has to be kept in mind that production of calcium oxide (temperature range 780 – 900oC) because of the decomposition of calcium carbonate had an unfavorable effect on the stoichiometry and phase of synthesized hydroxyapatite. The powder was dealt with 0.01 HCl along with greater temperature curing (>900oC) for developing the hydroxyapatite production and also to remove carbonates as well as residual CaO that is present in the system.

3.2.2 Agglomeration of Hydroxyapatite Particles Prepared by Precipitation Route

Saeri et.al produced stoichiometric hydroxyapatite through wet precipitation method by utilizing calcium hydroxyapatite and also orthophosphoric acid. The research was concentrated to analyze the result of response time and calcination temperature on the morphology of the incorporated

particle through field emission microscopy. The outcome disclosed that even though the precipitation technique could be considered to be an effective one compared to others because the precipitation continues during 'ageing time' but the precipitated particles are well agglomerated as visualized by the FE-SEM micrographs. The agglomeration tendency of the precipitates largely depended on ageing temperature and also on the ripening method and time.

Mobasherpour et.al used TEM (Transmission Electron Microscopy) and SEM (Scanning Electron Microscopy) to find out the particle size, morphology and agglomeration state of HAP incorporated through precipitation technique by using TEM and SEM. The SEM microstructure of HAP calcined at 1200oC stated the presence of big sized agglomerates produced of fine particles produced during drying. However, the TEM micrograph of the HAP stated particle size in the range from 40-50 nm. The processing technique had made a noteworthy development in the crystallinity of HAP .

3.2.3 Process modification for ensuring phase stability of Hydroxyapatite Prepared by Precipitation Route

Choi et.al incorporated chemical fortified hydroxyapatite through aqueous precipitation method utilizing CaCl2 and Na3PO4 as calcium and phosphorous origin respectively. NaOH was supplemented to make sure the accomplishment of precipitation response at ambient temperature. The XRD pattern statedd that the HAP produced by the supplementation of stoichiometric quantity of NaOH controlled the phase stability until1200oC as compared to other batch which were producedd through non stoichiometric quantity of NaOH. The variation of pH with time was observed in the case of batch that is not containing the NaOH. The ICP-OES (Inductively coupled plasma optical emission spectroscopy) result stated that with the supplement of stoichiometric quantity of NaOH, the ((Ca+Na)/P) ratio became 1.738 which is responsible for HAP to be more stable. Zhengwen et.al analysed the impact of microwave irradiation technique on the phase stability of precipitated HAP. The chore concentrated on the resultt of microwave irradiation time and power on the phase stability of HAP. The outcomes stated that the thermal stability of HAP raised with an rise in microwave radiation power and time along with ageing time. The microwave energy accelerated the motion of the molecules in the solution, and hence bettering the response rate with an attenuation of high Ca/P molar ratio in less time.

3.2.4 Preparation of Carbonated Apatite

Yanbao et.al formulated carbonate substituted amorphous HAP by utilizing ammonium carbonate (NH4)2CO3) and polyethylene glycol (PEG) with calcium nitrate hydrate ((CaNO3)2.4H2O) and ammonium hydrogen phosphate((NH4)2HPO4). The chemical composition of carbonated HAP being near to that of bone mineral was a subject of curiosity. The carbonated HAP stated even better biological properties and sinterability compared to pure HAP. The synthesized carbonated amorphous hydroxyapatite (Ca/P = 1.73) had nano sized particles and were highly clusterd. The primitive nano sized particle cluster on calcination at 800^{o}C was converted to carbonated HAP with the basic particle size of 50 nm. The development of primitive particles took place by the amalgam of cabonated crystalline hydroxyapatite.

3.2.5 Preparation of Hydroxyapatite by Biomimetic Route

A. Cuneyt Tas introduced a novel biomimetic synthesis method to produce Ca- HA. He used synthetic body fluid (SBF) solution instead of pure water at pH 7.4 and temperature 37oC. Calcium nitrate and di-ammonium hydrogen phosphate were utilized as the beginning material. The produced powder was phase stable till 1600oC without any decomposition of HA to β -TCP. This outcome was certainly different with that of others. Eventhough, minute quantity of organic ions were also introduced into the hydroxyapatite structure from the synthetic body fluid solution, it did not hamper the sintered density and the sintered samples had a relative density of ~ 96% on sintering at 1200oC for 6 hrs. The above mentioned studies recommends using of wet precipitation technique in yielding fine particles of crystalline HAP with better mechanical features. However, the disadvantages of this route, such as clustering tendency of the particles, low stoichiometry (due tolocalized precipitation) unfavorably disturbs the densification behavior and phase stability of the processed powders. On the other hand, techniques like sol-gel although produces a stoichiometric HAP but it is weakly crystallized which resulted in the weak mechanical features of such substances. Some research papers also recommended the advantages of microwave irradiation in restoring the phase stability of precipitated powder. Hence it could be concluded that wet precipitation method with some process modification could be accepted as an efficient, effective and cheaper way for the production of HAP .

CHAPTER – 4
RATIONALE AND SCOPE OF STUDY

RATIONALE AND SCOPE OF STUDY

For any project, the scope of study outlines the limitations of the research, the specific data used for the research and the theories used to interpret the data.

1) HYDROXYAPATITE

Many modern implants, e.g. hip substitutions, dental embeds and bone conduction inserts, are covered with hydroxylapatite. It has been proposed this may promote osseointegration. Permeable hydroxylapatite inserts are utilized for nearby medication conveyance in bone. It is likewise being utilized to repair early sores in tooth enamel.

2)ADVANTAGES

Despite alluring natural properties, hydroxylapatite, and materials based subsequently, have a few downsides, for example, low bioresorption rate in vivo, poor animating impact on the development of new bone tissues, low break resistance and little exhaustion strength in the physiological condition. The utilization of altered hydroxylapatite opens up the open doors for the planning of fake bone substances for inserts and an extensive assortment of medications for curing distinctive damage of bone, delicate and mucous tissues of the person.

3)PRACTICALITY

Companies that offer calcium hydroxyapatite refer to a few reviews to show its adequacy for bone wellbeing. HA has forestalled bone misfortune or expanded bone thickness in conjunction with medications in four reviews (Epstein, 1982, Pines, 1984, Castelo Branco 1999, Pelayo 2008,). It likewise expanded lower arm bone thickness when brought with professionally prescribed medications. 3000 milligrams of calcium hydroxyappatite every day expanded bone thickness in the lower arm in postmenopausal women (Fernandez-Parejo et al, 2007).

4)LIMITATION

Poor mechanical properties (fatigue properties) means that hydroxyapatite cannot be used in bulk form for load bearing applications such as orthopaedic.

CHAPTER-5

OBJECTIVES OF THE STUDY

OBJECTIVES OF THE STUDY

The work is divided into two parts.

1) In the first part, hydroxyapatite would be synthesized by heating the natural occurring sources such as oyster shells, egg shells, crab shells at high temperature and then by titrating it with acid and base HA would be formed.
2) To characterize by XRD, FTIR, SEM analysis of the raw shells and synthesized Hydroxyapatite as biomaterial available in different forms.

CHAPTER-6

MATERIALS AND METHODS

MATERIALS AND METHODS

6.1 SYNTHESIS OF HYDROXYAPATITE FROM OYSTER SHELLS

The raw oyster shells were taken and processed at high temperature in muffle furnace. It was set to 800^{o}C; which in turn converted the calcium carbonate into calcium oxide. Calcium oxide ($CaCO_3$) when absorbs moisture it got converted into calcium hydroxide ($Ca(OH)_2$). When calcium hydroxide is treated with orthophosphoric acid (H_3PO_4) it produced hydroxyapatite ($Ca_5(PO_4)_6(OH)_2$) and water (H_2O). It worked by a general phenomena i.e when base and acid reacts it gives rise to salt and water. In the same way the HA synthesis was done.

Take oyster shells

Place it in beaker filled with water for 10 minutes

Rinse off the water and dry the shells

Shells are placed in hot air oven at 160 ^{o}C for 5 minutes

Put the shells in the crucibles

Keep the crucibles in the furnace

Set the temperature of the furnace at 800 ^{o}C for 2 hours

Measure the weight of the calcium carbonate formed after heating the shells

Crush the shells in mortar with the help of pestle

Grind it in a mixer till fine powder is formed

Again weight the powder formed

Take a sample of the powder and do FTIR

Take the sample of the calcium hydroxide powder from lab and do FTIR, SEM and XRD

Analyze the difference in the graphs formed from FTIR

Analyze the difference in graph formed from XRD

Analyze the images formed from SEM

Figure 6.1.1 : Flow chart representation for $Ca(OH)_2$ formation from oyster shells

Steps involved in the formation of HA formation from oyster shells:

- 0.5M 100 ml ammonia (NH_3) was taken for HA formation.

  [0.5=Mass(x)/M.W * 1000/100], where molecular weight (M.W) = 74.09

  Mass(x) = 3.7045g

- 0.3M 100ml ortho phosphoric acid (H_3PO_4) which is an acid was taken for HA formation.

  [0.3=Mass(x)/M.W * 1000/100], where molecular weight (M.W) = 98

  Mass(x) = 2.94ml

- 3.7045 gm of $Ca(OH)_2$ was taken in a beaker and making it up to 100 ml by adding ammonia solution and was left overnight.

- The next day titration was done by taking the beaker containing $Ca(OH)_2$ and basic solution ammonia and in the burette 2.94 ml of orthophosphoric acid was added and it was made up to 100 ml by adding distilled water. Hence salt was formed which is hydroxyapatite (HA).

$$5Ca(OH)_2 + 3H_3PO_4 \qquad Ca_5(PO_4)_6(OH)_2 + 9H_2O$$

BASE + ACID SALT (HA) + WATER

- Several times washing was done and then the salt that is left in the beaker was kept for some time in hot air oven to dry and then it was collected and crushed to fine powder which resulted in the formation of HA.

- 1g of HA was taken in an eppendorf for FTIR analysis.

Oyster shells were collected from the sea shore of eastern coastal region of Odisha state. The name of the sea shore is Gopalpur sea beach. It is 18 kms far from Berhampur city of Ganjam district.

Figure 6.1.2 : represents oyster shells

The oyster shells were taken and washed several times and then placed it in a beaker and poured water on it and left for 10 minutes to remove dust and dirt that was present on the surface of the shells.

Figure 6.1.3 : represents oyster shells placed in a beaker filled with water

The water was poured out from the beaker and was left for some time to dry. Then the beaker

with shells was placed inside the hot air oven where the temperature was maintained at 160°C for 5 minutes.

(a) **(b)**

Figure 6.1.4 : (a) and (b) represents hot air oven and the controlled temperature respectively

The oyster shells were taken and weighed through a weighing machine and the value was noted that was being displayed. The weight displayed was 101.780 grams

Figure 6.1.5 : represents weight of the oyster shells

Crucibles were taken and were washed thoroughly. Then it was left for some time to dry. Oyster shells were placed in the crucibles

Figure 6.1.6 : represents clean and empty crucibles

Figure 6.1.7: represents oyster shells placed in crucibles

The high heat resistant crucibles were now placed in the muffle furnace for the calcification of the shells. The calcification was done at 800°C for 2 hours so that calcium carbonate could be converted into calcium oxide. The temperature was controlled manually.

(a) **(b)**

Figure 6.1.8 : (a) and (b) represents muffle furnace and crucibles placed in furnace respectively

Figure 6.1.9: represents the furnace is working at a temperature of 800°C

6.2 SYNTHESIS OF HYDROXYAPETITE FROM EGG SHELLS

The raw egg shells were taken and processed at high temperature in muffle furnace. It was set to 800^{o}C; which in turn converted the calcium carbonate into calcium oxide. Calcium oxide ($CaCO_3$) when absorbs moisture it got converted into calcium hydroxide ($Ca(OH)_2$). When calcium hydroxide is treated with orthophosphoric acid (H_3PO_4) it produced hydroxyapatite ($Ca_5(PO_4)_6(OH)_2$) and water (H_2O). It worked by a general phenomena i.e when base and acid reacts it gives rise to salt and water. In the same way the HA synthesis was done.

Take egg shells

Place it in beaker filled with water for 10 minutes

Rinse off the water and dry the shells

Shells are placed in hot air oven at 160 oC for 5 minutes

Put the shells in the crucibles

Keep the crucibles in the furnace

Set the temperature of the furnace at 800 oC for 2 hours

Measure the weight of the calcium carbonate formed after heating the shells

Crush the shells in mortar with the help of pestle

Grind it in a mixer till fine powder is formed

Again weigh the amount of powder formed

Take a sample of the powder and do FTIR

Take a sample of the calcium hydroxide powder from lab and do FTIR

Analyze the difference in the graphs formed

Take the powder formed, ammonia and orthophosphoric acid for titration; where base and acid reacts to form salt which is HA

Take a sample of the HA for FTIR, XRD and SEM analysis and study the features.

Analyze the difference in graphs formed formed FTIR

Analyze the difference in graphs formed from XRD

Analyze the difference in images formed from SEM

Figure 6.2.1 : Flow chart representation for Ca(OH)2 formation from egg shells

Steps involved in the formation of HA formation from egg shells:

- 0.5M 100 ml ammonia (NH_3) was taken for HA formation.

  [0.5=Mass(x)/M.W * 1000/100], where molecular weight (M.W) = 74.09

  Mass(x) = 3.7045g

- 0.3M 100ml ortho phosphoric acid (H_3PO_4) which is an acid was taken for HA formation.

  [0.3=Mass(x)/M.W * 1000/100], where molecular weight (M.W) = 98

  Mass(x) = 2.94ml

- 3.7045 gm of Ca(OH)2 was taken in a beaker and making it up to 100 ml by adding ammonia solution and was left overnight.

- The next day titration was done by taking the beaker containing Ca(OH)2 and basic solution ammonia and in the burette 2.94 ml of orthophosphoric acid was added and it was made up to 100 ml by adding distilled water. Hence salt was formed which is hydroxyapatite (HA).

$$5Ca(OH)_2 + 3H_3PO_4 \qquad Ca_5(PO_4)_6(OH)_2 + 9H_2O$$

BASE + ACID SALT (HA) + WATER

- Several times washing was done and then the salt that is left in the beaker was kept for some time in hot air oven to dry and then it was collected and crushed to fine powder which resulted in the formation of HA.

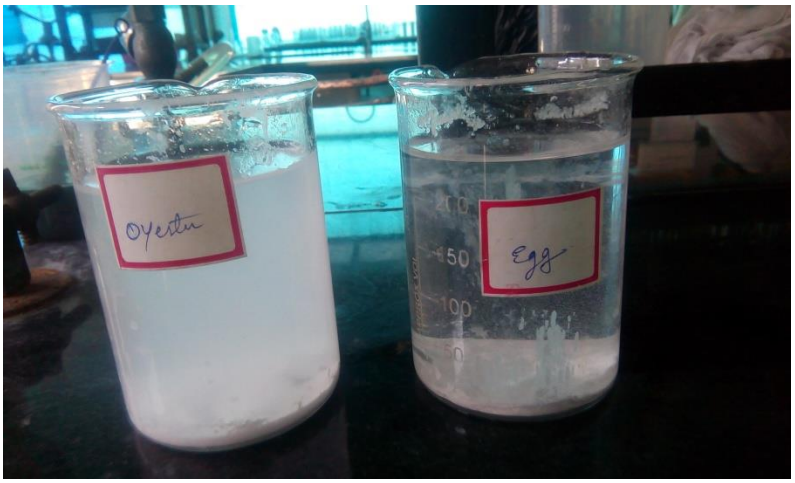

Figure 6.2.2 : represents HA formed at the bottom of the beakers from oyster and egg shells respectively

- 1g of HA was taken in an eppendorf for FTIR analysis.

  The egg shells were collected from the egg selling vendors near Lovely Professional University. The egg shells were already broken into small pieces while collecting.

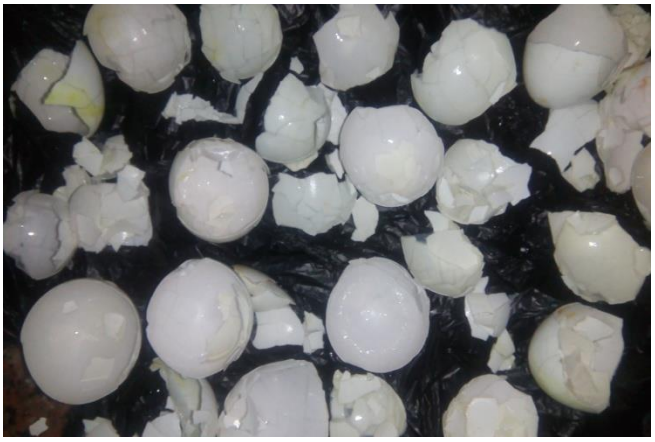

Figure 6.2.3 : represents broken egg shells

The egg shells were taken and placed in a beaker and poured water on it and left for 10 minutes to remove dirt and then dried it by placing the beaker in hot air oven at 160^{o}C for 5 min

(a) **(b)** **(c)**

Figure 6.2.4 : (a), (b) and (c) represents egg shells placed in a beaker, the beaker placed in hot air oven and the temperature is set at 160°C respectively

After taking out the shells from hot air oven the shells were placed in crucibles which can resist at higher temperature and then was kept in muffle furnace for calcinations and the temperature was maintained abou 800°C for 2 hours.

(a) **(b)** **(c)**

Figure 6.2.5 : (a), (b) and (c) represents the egg shells placed in crucibles, the crucibles are placed in furnace and the temperature is set to 800°C

6.3 SYNTHESIS OF HYDROXYAPATITE FROM CRAB SHELLS

The raw crab shells were taken and processed at high temperature in muffle furnace. It was set to 800^{o}C; which in turn converted the calcium carbonate into calcium oxide. Calcium oxide ($CaCO_3$) when absorbs moisture it got converted into calcium hydroxide ($Ca(OH)_2$). When calcium hydroxide is treated with orthophosphoric acid (H_3PO_4) it produced hydroxyapatite ($Ca_5(PO_4)_6(OH)_2$) and water (H_2O). It worked by a general phenomena i.e when base and acid reacts it gives rise to salt and water. In the same way the HA synthesis was done.

Take crab shells and break it into pieces

Place it in beaker filled with water for 10 minutes

Rinse off the water and dry the shells

Shells are placed in hot air oven at 160 oC for 5 minutes

Put the shells in the crucibles

Keep the crucibles in the furnace

Set the temperature of the furnace at 800 oC for 2 hours

Measure the weight of the calcium carbonate formed after heating the shells

Crush the shells in mortar with the help of pestle

Grind it in a mixer till fine powder is formed

Again weigh the amount of powder formed

Take a sample of the powder and do FTIR

Take a sample of the calcium hydroxide powder from lab and do FTIR

Analyze the difference in the graphs formed

Take the powder formed, ammonia and orthophosphoric acid for titration; where base and acid reacts to form salt which is HA

Take a sample of the HA for FTIR, XRD and SEM and analysis and study the features

Analyze the difference in graphs formed from FTIR

Analyze the difference in graphs formed from XRD

Analyze the difference in graphs formed from SEM

Figure 6.3.1 : Flow chart representation for Ca(OH)2 formation from crab shells

Steps involved in the formation of HA formation from crab shells:

- 0.5M 100 ml ammonia (NH_3) was taken for HA formation.

  [0.5=Mass(x)/M.W * 1000/100], where molecular weight (M.W) = 74.09

  Mass(x) = 3.7045g

- 0.3M 100ml ortho phosphoric acid (H_3PO_4) which is an acid was taken for HA formation.

  [0.3=Mass(x)/M.W * 1000/100], where molecular weight (M.W) = 98

  Mass(x) = 2.94ml

- 3.7045 gm of Ca(OH)2 was taken in a beaker and making it up to 100 ml by adding ammonia solution and was left overnight.

- The next day titration was done by taking the beaker containing Ca(OH)2 and basic solution ammonia and in the burette 2.94 ml of orthophosphoric acid was added and it was made up to 100 ml by adding distilled water. Hence salt was formed which is hydroxyapatite (HA).

$$5Ca(OH)_2 + 3H_3PO_4 \qquad Ca_5(PO_4)_6(OH)_2 + 9H_2O$$

BASE + ACID SALT (HA) + WATER

- Several times washing was done and then the salt that is left in the beaker was kept for some time in hot air oven to dry and then it was collected and crushed to fine powder which resulted in the formation of HA.

(a) **(b)**

Figure 6.3.2 : (a) and (b) represents HA formed at the bottom of the beakers

- 1g of HA was taken in an eppendorf for FTIR analysis.

Crab shells were collected from the sea shore of eastern coastal region of Odisha state. . The name of the sea shore is Baleswar sea beach.

Figure 6.3.3 : represents crab shells

The shells were rich in calcium carbonate and chitin so directly some pieces of shell were taken and fine powder was made out of it and a small sample was given for FTIR analysis.

The crab shells were taken and placed in a beaker and poured water on it and left for 10 minutes to remove dirt and then dried it by placing the beaker in hot air oven at 160^{o}C for 5 min

Figure 6.3.4 : represents crab shells were broken into small pieces and placed in a beaker filled with water

After taking out the shells from hot air oven the shells were placed in crucibles which can resist at higher temperature and then was kept in muffle furnace for calcinations and the temperature was maintained abou 800^{o}C for 2 hours.

Figure 6.3.5 : represents pieces of crab shells placed in crucibles

After the processing in furnace, the calcium oxide absorbs moisture and turns into calcium hydroxide and fine powder was made of it. A sample of it was given for FTIR analysis

6.4 FTIR ANALYSIS

FT-IR Spectrometers are frequently just called FTIRs. Be that as it may, for the idealists, a FT-IR (Fourier Transform InfraRed) is a technique for acquiring infrared spectra by essential gathering an interferogram of a specimen flag utilizing an interferometer, and afterward playing out a Fourier Transform (FT) on the interferogram to get the range. A FT-IR Spectrometer gathers and digitizes the interferogram, plays out the FT work, and shows the range.

Components for working of a FTIR:

- Sample
- Source
- Moving mirror and Beam splitter
- Laser
- Detector
- Interferometer
- Computer

A FT-IR is completely in light of The Michelson Interferometer Experimental Setup. The interferometer is comprised of a pillar splitter, a settled mirror, and a mirror that interprets forward and backward, unequivocally. The bar splitter comprises of an uncommon material that transmits half of the radiation striking it and mirrors the other half. Radiation from the source strikes the pillar splitter and isolates into two shafts. One bar is transmitted through the bar splitter to the settled mirror and the second is reflected off the shaft splitter to the moving mirror. The settled and moving mirrors mirror the radiation back to the beamsplitter. Once more, half of this reflected radiation is transmitted and half is reflected at the pillar splitter, bringing about one bar going to the identifier and the second back to the source.

6.5 **XRD ANALYSIS**

X-beam powder diffraction (XRD) is a quick analytical strategy essentially utilized for stage distinguishing proof of a crystalline material and can give data on unit cell measurements. The examined material is finely ground, homogenized, and average bulk composition is resolved.

Components of a XRD Diffractometer

- X-ray tube
- Goniometer and optical path
- Sample Holder
- Detector

X-beams are created in a cathode beam tube by warming a fiber to deliver electrons, quickening the electrons toward an objective by applying a voltage, and shelling the objective material with electrons. At the point when electrons have adequate vitality to remove internal shell electrons of the objective material, trademark X-beam spectra are created. These spectra comprise of a few parts, the most widely recognized being Kα and Kβ. Kα comprises, to a limited extent, of Kα1 and Kα2. Kα1 has a somewhat shorter wavelength and double the force as Kα2. The particular wavelengths are normal for the objective material (Cu, Fe, Mo, Cr). Separating, by foils or gem monochrometers, is required to create monochromatic X-beams required for diffraction. Kα1and Kα2 are adequately close in wavelength with the end goal that a weighted normal of the two is utilized. Copper is the most widely recognized target material for single-precious stone diffraction, with CuKα radiation = 1.5418å. These X-beams are collimated and coordinated onto the example. As the example and identifier are turned, the force of the reflected X-beams is recorded. At the point when the geometry of the episode X-beams impinging the example fulfills the Bragg Equation, helpful impedance happens and a top in power happens. A locator records and procedures this X-beam flag and changes over the flag to a tally rate which is then yield to a gadget, for example, a printer or PC screen**.**

6.6 SEM ANALYSIS

SEM is Scanning Electron Microscopy. It is a kind of electron magnifying lens which helps in making pictures of an analyte by the particular component of filtering of electrons in a focussed shaft. The connection of electrons with molecules in the example, delivering different signs that contain data about the specimen's surface geology and organization. SEM can accomplish determination superior to 1 nanometer. Examples can be seen in high vacuum, in low vacuum and at an extensive variety of cryogenic or hoisted temperatures.

COMPONENTS OF SEM

- Electron Source
- Lenses
- Scanning Coil
- Sample Chamber
- SEM Detectors

Accelerateded electrons in a SEM convey critical measures of dynamic vitality, and this vitality is disseminated as an assortment of signs created by electron-test communications when the occurrence electrons are decelerated in the strong example. These signs incorporate auxiliary electrons (that deliver SEM pictures), backscattered electrons (BSE), diffracted backscattered electrons, noticeable light (cathodoluminescence–CL), and warmth. Optional electrons and backscattered electrons are normally utilized for imaging tests: auxiliary electrons are most important for indicating morphology and geography on tests and backscattered electrons are most significant for representing contrasts in organization in multiphase specimens (i.e. for quick stage separation). X-beam era is delivered by inelastic impacts of the occurrence electrons with electrons in discrete orbitals (shells) of molecules in the specimen. As the energized electrons come back to lower vitality states, they yield X-beams that are of a settled wavelength. Consequently, trademark X-beams are created for every component in a mineral that is "energized" by the electron pillar. SEM investigation is thought to be "non-ruinous"; that is, x-beams created by electron associations don't prompt volume loss of the specimen, so it is conceivable to break down similar materials over and again

CHAPTER – 7

RESULTS AND EXPERIMENTAL WORK

7.1 HYDROXYAPATITE FROM OYESTER SHELLS

The calcined shells were collected and it has turned to calcium oxide then to calcium hydroxide by absorbing moisture from the surrounding area. To turn it into powder mortar and pestle were used and even to make it more fine grinder was used to make it amorphous.

(a) **(b)**

Figure 7.1.1 : (a) and (b) represents oyster shells after calcination were crushed by using mortar and pestle and amorphous powder was produced using grinder

The amount of calcium oxide that converted into calcium hydroxide powder formed from those shells after calcination at 800^{o}C for 2 hours was weighed. The weight it displayed was 57.2461g

Figure 7.1.2 : represents weight of powder formed using weighing machine

The powder was stored safely for further procedures.The powder was further analyzed by FTIR which is Fourier Transform Infrared Spectrometry.

Figure 7.1.3 : represents storage of Ca(OH)2 powder in a conical flask.

1g of calcium hydroxide was taken in an eppendorf formed from oyster shells for FTIR analysis.FTIR is fourier transform Infrared Spectroscopy, where the infrared region of light is used to analyze the peaks of the bonds and stretch of the molecule.

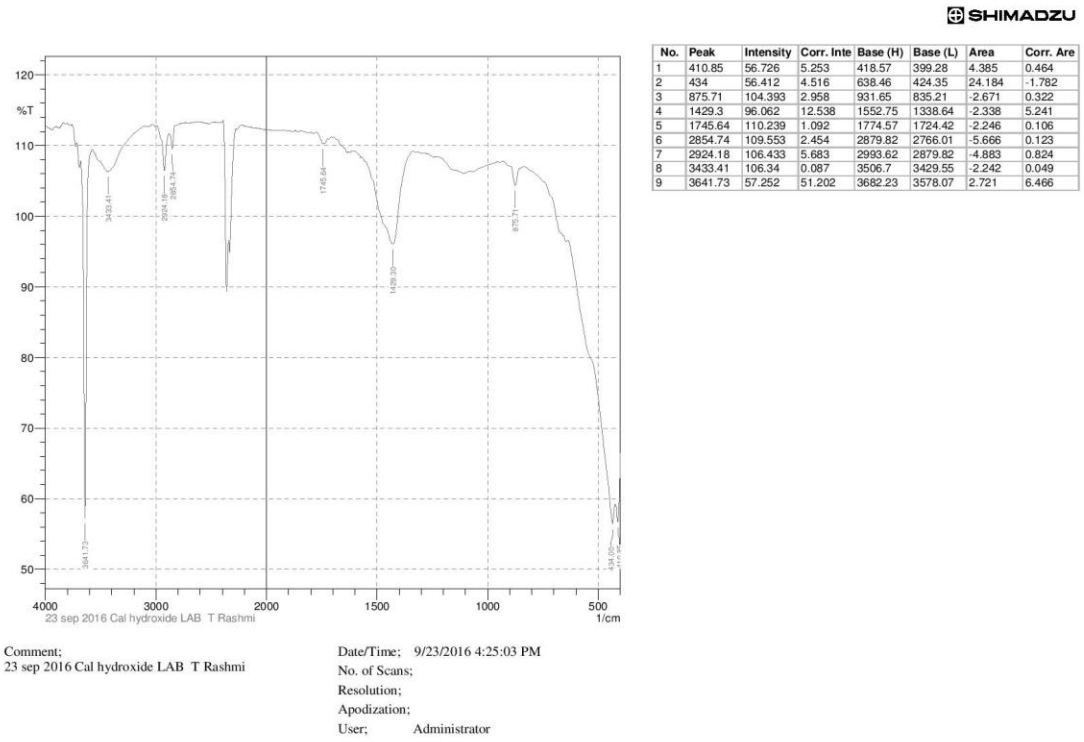

No.	Peak	Intensity	Corr. Inte	Base (H)	Base (L)	Area	Corr. Are
1	410.85	56.726	5.253	418.57	399.28	4.385	0.464
2	434	56.412	4.516	638.46	424.35	24.184	-1.782
3	875.71	104.393	2.958	931.65	835.21	-2.671	0.322
4	1429.3	96.062	12.538	1552.75	1338.64	-2.338	5.241
5	1745.64	110.239	1.092	1774.57	1724.42	-2.246	0.106
6	2854.74	109.553	2.454	2879.82	2766.01	-5.666	0.123
7	2924.18	106.433	5.683	2993.62	2879.82	-4.883	0.824
8	3433.41	106.34	0.087	3506.7	3429.55	-2.242	0.049
9	3641.73	57.252	51.202	3682.23	3578.07	2.721	6.466

Figure 7.1.4 : FTIR of standardized $Ca(OH)_2$ taken from laboratory

FTIR ANALYSIS OF STANDARD $Ca(OH)_2$ FTIR GRAPH :

Figure 7.1.4 represents that the standardized calcium hydroxide was was analyzed under FTIR. There were several peaks observed which confirmed about the type and nature of molecules including peaks, intensity, correlation area and many more. The wave number 875.71cm^{-1} showed the presence of aromatic C-H bending, 1429.3cm^{-1} wave nuber revealed the presence of alkane (-C-H) functional group,and the intensity was variable.1745.64cm^{-1} wave number showed ester C=O stretch, 2854.74cm^{-1} described about the alkyl C-H stretch, it is fairly ubiquitous and is usually less useful in determining the structure. 2924.18cm^{-1} wave number showed carboxylic acid O-H stretch and finally 3641.73cm^{-1} wave number peak told about the amide N-H stretch ,an amide produces zero to two N-H absorptions depending on its types [Silverstein, R.M *et al.*, 1981]

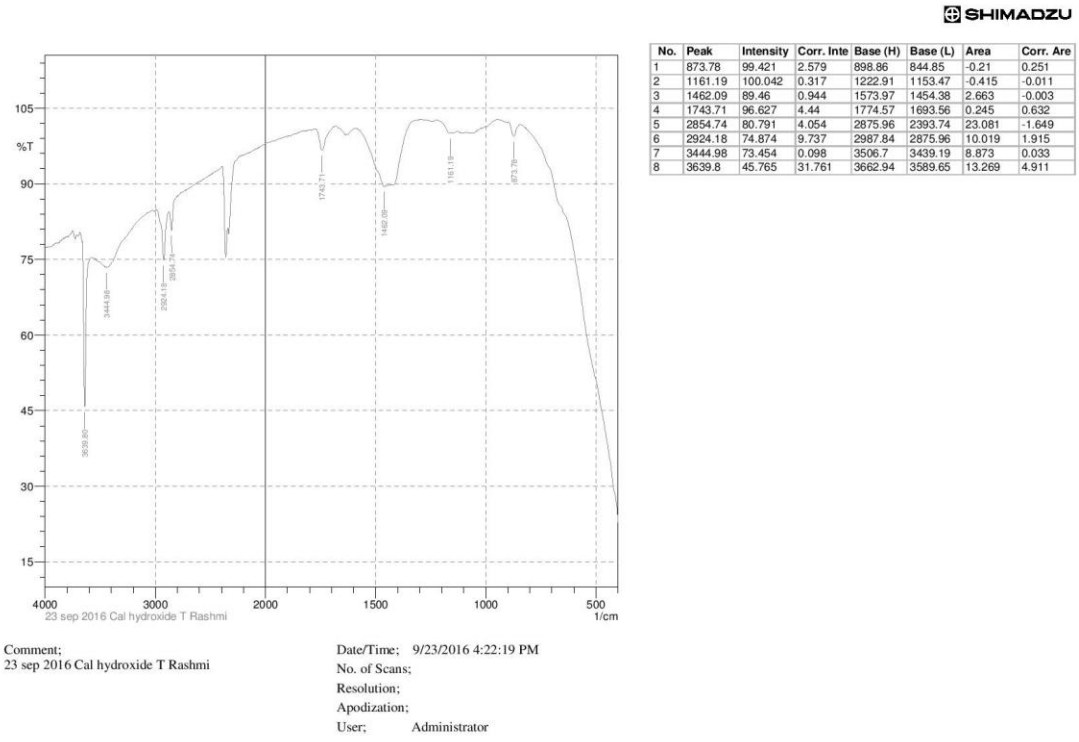

No.	Peak	Intensity	Corr. Inte	Base (H)	Base (L)	Area	Corr. Are
1	873.78	99.421	2.579	898.86	844.85	-0.21	0.251
2	1161.19	100.042	0.317	1222.91	1153.47	-0.415	-0.011
3	1462.09	89.46	0.944	1573.97	1454.38	2.663	-0.003
4	1743.71	96.627	4.44	1774.57	1693.56	0.245	0.632
5	2854.74	80.791	4.054	2875.96	2393.74	23.081	-1.649
6	2924.18	74.874	9.737	2987.84	2875.96	10.019	1.915
7	3444.98	73.454	0.098	3506.7	3439.19	8.873	0.033
8	3639.8	45.765	31.761	3662.94	3589.65	13.269	4.911

Figure 7.1.5 : FTIR of $Ca(OH)_2$ formed after processing (calcination) of oyster shells

FTIR ANALYSIS OF $Ca(OH)_2$ PRODUCED FROM OYSTER SHELLS

Figure 7.1.5 represents that the calcium hydroxide formed from calcinations of oyster shells at 800oC was analyzed under FTIR. It revealed about several bending and stretching of the molecules in the form of peaks present in calcium hydroxide from oyster shells. 873.78cm^{-1} wave number showed the presence of aromatic C-H bending. 1161.19cm^{-1} revealed the presence of an alky functional group. 1462.09cm^{-1} wave number described about the presence of alkane (-C-H) whose intensity is variable. 1743.71cm^{-1} wave number told about the ester C=O stretch. 2854.74cm^{-1} wave number peak showed alkyl C-H stretch, it is fairly ubiquitous and is usually less useful in determining the structure. 2924.18cm^{-1} wave number resulted in the presence of carboxylic acid O-H stretch and finally 3444cm^{-1} wave number mentioned the presence of amideN-H stretch [Silverstein, R.M *et al.*, 1981].

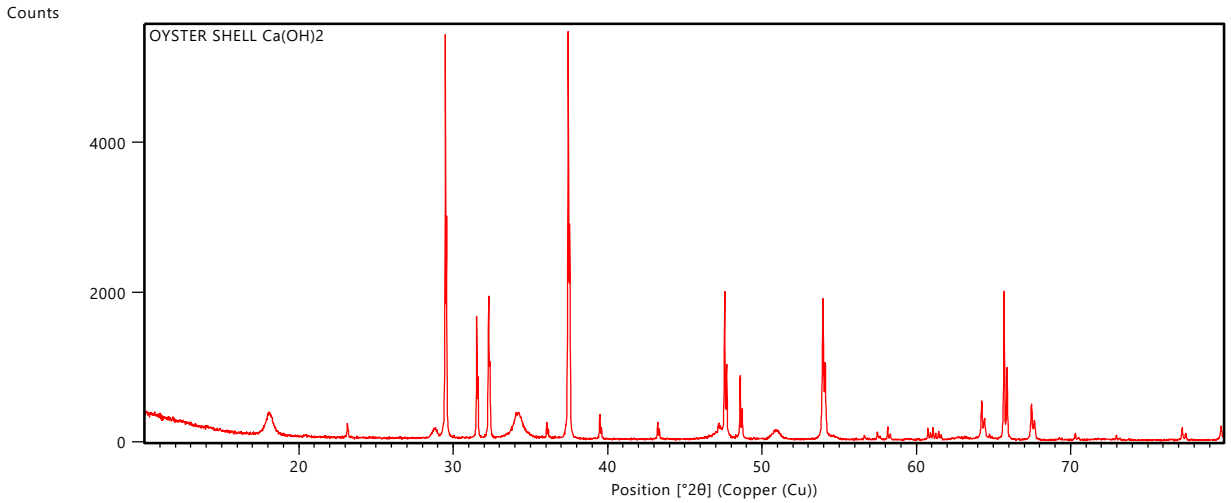

Figure 7.1.6: represents XRD of Ca(OH)2 formed after processing of oyster shells

Dataset Name	OYSTER SHELL Ca(OH)2
File name	C:\XRD Data\APRIL l2017\OYSTER SHELL Ca(OH)2.xrdml
Sample Identification	OYSTER SHELL Ca(OH)2
Comment	Configuration=Reflection Spinner Stage, Owner=User-1, Creation date=20-09-2016 16:48:22

Goniometer=PW3050/60 (Theta/Theta); Minimum step size 2Theta:0.001; Minimum step size Omega:0.001

Sample stage=Spinner PW3064

Diffractometer system=XPERT-PRO

Measurement program=C:\PANalytical\Data Collector\Programs\Spinner.xrdmp, Identifier={544E0168-3858-47A1-AD8C-A5C91B0E4D3F}

Batch program=C:\PANalytical\Data Collector\Progams\SPINNER-1.xrdmp, Identifier={C20B4B02-C535-42F0-ADD7-4D3DF73E7C16}

PHD Lower Level = 6.52 (keV), PHD Upper Level = 12.80 (keV)

Measurement Start Date/Time	25-04-2017 13:49:06
Operator	User
Raw Data Origin	XRD measurement (*.XRDML)
Scan Axis	Gonio
Start Position [°2θ]	10.0084
End Position [°2θ]	79.9804
Step Size [°2θ]	0.0170
Scan Step Time [s]	29.8450
Scan Type	Continuous
PSD Mode	Scanning
PSD Length [°2θ]	2.12
Offset [°2θ]	0.0000
Divergence Slit Type	Fixed
Divergence Slit Size [°]	0.8709
Specimen Length [mm]	10.00
Measurement Temperature [°C]	25.00
Anode Material	Cu
K-Alpha1 [Å]	1.54060
Generator Settings	40 mA, 45 kV
Diffractometer Type	0000000011023505
Diffractometer Number	0
Goniometer Radius [mm]	240.00
Dist. Focus-Diverg. Slit [mm]	100.00

Incident Beam Monochromator No

Spinning Yes

Pos. [°2θ]	FWHM Left [°2θ]	d-spacing [Å]	Rel. Int. [%]	Area [cts*°2θ]
10.2430	0.4015	8.62908	1.60	34.99
18.0202	0.2007	4.91862	5.02	55.03
23.1252	0.0836	3.84307	3.29	15.05
28.7944	0.2342	3.09802	2.35	30.07
29.4902	0.0408	3.02648	98.85	297.78
31.5216	0.0612	2.83592	27.57	124.59
32.2938	0.0816	2.76985	34.64	208.68
34.1561	0.6528	2.62297	6.13	295.27
36.0634	0.0612	2.48850	4.10	18.51
37.4463	0.0612	2.39972	100.00	451.87
39.4997	0.0612	2.27957	5.92	26.77
43.2460	0.0612	2.09038	4.24	19.16
47.1850	0.0816	1.92464	3.42	20.61
47.5866	0.0612	1.90934	36.99	167.16
48.5880	0.0612	1.87230	15.57	70.37
50.9567	0.5712	1.79068	2.13	90.03
53.9506	0.0816	1.69816	34.51	207.90
56.6507	0.1224	1.62347	0.83	7.51
57.4788	0.0612	1.60203	1.82	8.22
58.1585	0.0612	1.58492	3.21	14.50
60.7583	0.0612	1.52317	2.89	13.07

61.0865	0.0612	1.51577	3.02	13.65
61.4512	0.0816	1.50765	2.05	12.35
64.2451	0.0816	1.44866	9.61	57.87
65.6919	0.0612	1.42021	37.89	171.20
67.4669	0.1020	1.38710	8.83	66.48
70.3052	0.0816	1.33789	1.59	9.57
72.9627	0.1224	1.29558	1.00	9.05
77.2282	0.0816	1.23431	3.05	18.40
79.7447	0.1020	1.20157	3.37	25.39

XRD ANALYSIS OF $Ca(OH)_2$ PRODUCED FROM OYSTER SHELL

The high intensity peaks were observed was 2ɵ at 29.4^o and 37.44^o.The relative intensity were 98.85% and 100% respectively. The scanning angle was set from 10^o to 80^o. The crystalline phase identified was JCPD, 4-0733.

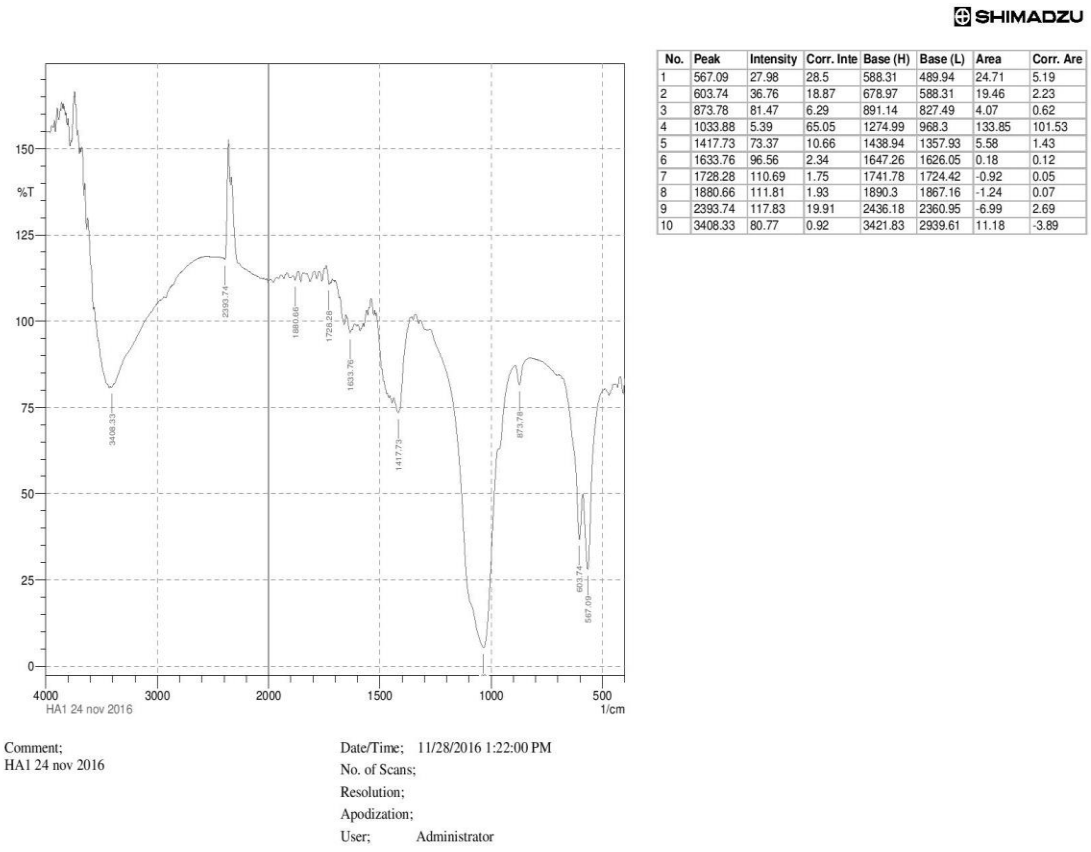

No.	Peak	Intensity	Corr. Inte	Base (H)	Base (L)	Area	Corr. Are
1	567.09	27.98	28.5	588.31	489.94	24.71	5.19
2	603.74	36.76	18.87	678.97	588.31	19.46	2.23
3	873.78	81.47	6.29	891.14	827.49	4.07	0.62
4	1033.88	5.39	65.05	1274.99	968.3	133.85	101.53
5	1417.73	73.37	10.66	1438.94	1357.93	5.58	1.43
6	1633.76	96.56	2.34	1647.26	1626.05	0.18	0.12
7	1728.28	110.69	1.75	1741.78	1724.42	-0.92	0.05
8	1880.66	111.81	1.93	1890.3	1867.16	-1.24	0.07
9	2393.74	117.83	19.91	2436.18	2360.95	-6.99	2.69
10	3408.33	80.77	0.92	3421.83	2939.61	11.18	-3.89

Figure 7.1.7 : FTIR of HA formed from oyster shells

FTIR ANALYSIS OF HA FTIR GRAPH PRODUCED FROM OYSTER SHELLS

Figure 7.1.6 represents that the Hydroxyapatite produced by chemically treating the calcium hydroxide produced from oyster shells was analyzed through FTIR. The report showed the peaks which revealed the presence of several functional groups with their bending and stretching properties. 567.09cm^{-1}, 603.74cm^{-1} and 1033.88cm^{-1} wave number showed the presence of alkyl functional group. 873.78cm^{-1} and1417.73cm^{-1} wave number described about the presence of aromatic C-H bending. 1633.76cm^{-1} wave number resulted in the presence of aromatic C=C bending.1728.28cm^{-1} and 1880,66cm^{-1} wave number stated the presence of ester C=O stretch. Finally 2393.74cm^{-1} and 3408.33cm^{-1} wave number showed the presence of O-H stretch [Silverstein, R.M *et al.*, 1981].

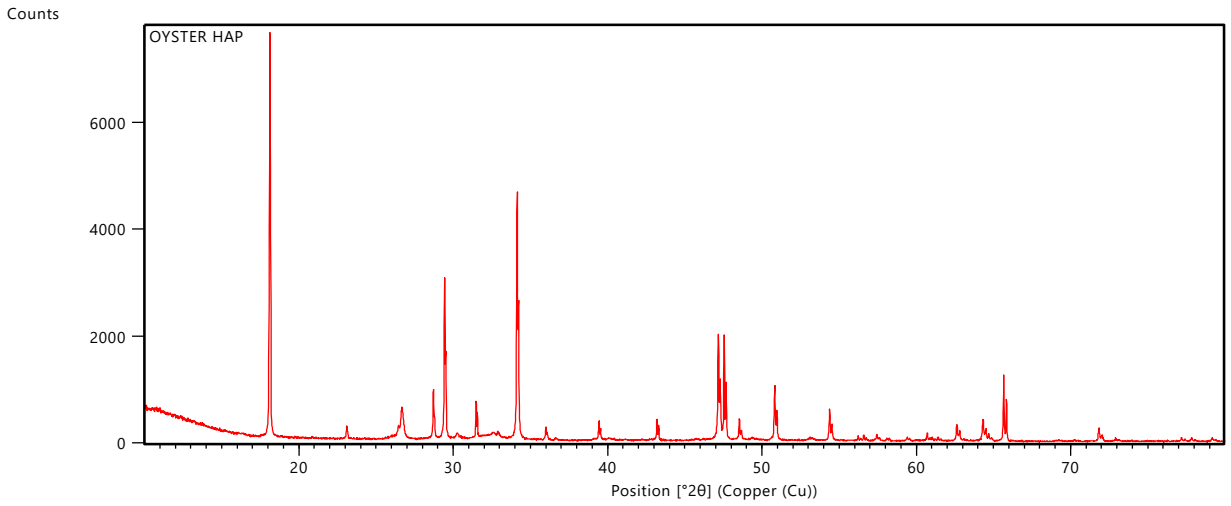

Figure 7.1.8: XRD of HA formed from oyster shells

Dataset Name	OYSTER HAP
File name	C:\XRD Data\APRIL l2017\OYSTER HAP.xrdml
Sample Identification	OYSTER HAP
Comment	Configuration=Reflection Spinner Stage, Owner=User-1, Creation date=20-09-2016 16:48:22

Goniometer=PW3050/60 (Theta/Theta); Minimum step size 2Theta:0.001; Minimum step size Omega:0.001

Sample stage=Spinner PW3064

Diffractometer system=XPERT-PRO

Measurement program=C:\PANalytical\Data Collector\Programs\Spinner.xrdmp, Identifier={544E0168-3858-47A1-AD8C-A5C91B0E4D3F}

Batch program=C:\PANalytical\Data Collector\Programs\SPINNER-1.xrdmp, Identifier={C20B4B02-C535-42F0-ADD7-4D3DF73E7C16}

PHD Lower Level = 6.52 (keV), PHD Upper Level = 12.80 (keV)

Measurement Start Date/Time	25-04-2017 13:30:33

Operator	User
Raw Data Origin	XRD measurement (*.XRDML)
Scan Axis	Gonio
Start Position [°2θ]	10.0084
End Position [°2θ]	79.9804
Step Size [°2θ]	0.0170
Scan Step Time [s]	29.8450
Scan Type	Continuous
PSD Mode	Scanning
PSD Length [°2θ]	2.12
Offset [°2θ]	0.0000
Divergence Slit Type	Fixed
Divergence Slit Size [°]	0.8709
Specimen Length [mm]	10.00
Measurement Temperature [°C]	25.00
Anode Material	Cu
K-Alpha1 [Å]	1.54060
Generator Settings	40 mA, 45 kV
Diffractometer Type	0000000011023505
Diffractometer Number	0
Goniometer Radius [mm]	240.00
Dist. Focus-Diverg. Slit [mm]	100.00
Incident Beam Monochromator	No
Spinning	Yes

Pos. [°2θ]	FWHM Left [°2θ]	d-spacing [Å]	Rel. Int. [%]	Area [cts*°2θ]
18.1065	0.0836	4.89539	100.00	641.82
23.0868	0.0669	3.84937	3.25	16.67
26.6329	0.1171	3.34434	7.13	64.03
28.6912	0.0502	3.10893	12.19	46.94
29.4406	0.0612	3.03147	40.14	254.79
30.2686	0.2040	2.95040	1.58	33.42
31.4823	0.0408	2.83938	9.73	41.18
32.9139	0.2040	2.71907	1.70	35.98
34.1384	0.0612	2.62429	59.75	379.28
36.0097	0.0612	2.49209	3.16	20.03
39.4442	0.0612	2.28265	4.76	30.21
43.1974	0.0612	2.09262	5.38	34.13
47.1793	0.0816	1.92487	26.46	223.96
47.5510	0.0612	1.91068	26.22	166.41
48.5344	0.0612	1.87424	5.22	33.15
50.8317	0.0816	1.79479	13.31	112.66
53.1659	0.2448	1.72136	0.55	13.88
54.3882	0.0816	1.68553	7.73	65.45
56.2409	0.0612	1.63432	1.27	8.05
56.6099	0.0816	1.62454	1.38	11.70
57.4480	0.0612	1.60282	1.47	9.34
58.1711	0.2448	1.58460	0.38	9.66
59.4136	0.0816	1.55440	0.99	8.36
60.7129	0.0612	1.52420	1.91	12.09

61.4099	0.0816	1.50856	0.92	7.77
62.6338	0.1020	1.48200	4.10	43.38
64.3284	0.0816	1.44699	5.42	45.91
64.7009	0.0816	1.43955	1.83	15.47
65.6660	0.0816	1.42071	16.10	136.28
69.1868	0.4896	1.35676	0.23	11.53
70.2989	0.4896	1.33800	0.20	10.06
71.8354	0.0816	1.31311	3.39	28.68
73.0002	0.4080	1.29500	0.41	17.32
77.1804	0.0816	1.23496	0.95	8.03
77.8342	0.1224	1.22621	0.76	9.65
79.1639	0.1224	1.20892	0.77	9.82

XRD ANALYSIS OF HA FTIR GRAPH PRODUCED FROM OYSTER SHELLS

From the XRD graph of the sample, irregular spectrum was observed with increase in sintering time. Three high intensity peaks located at 2ɵ is 18.1^{o}, 34.13^{o} and 29.44^{o} with Cu-Kα radiation are hard to be precisely perceived from their diffraction designs. XRD designs uncovers the development of HAP and is all around taken after with the standard JCPDS document. The unindexed top at 34.13 might be expected to β-tricalcium phosphate; which demonstrates the start of change of HAP to β-tricalcium phosphate on warming HAP over 800°C. The calcined HAP shows very much solidified sharp pinnacles of attributes HAP. The HAP powders, in this manner combined from Oyster Shell forerunner, are exceptionally immaculate and concoction examination of powders affirms a similar perception. HA. As already said, the Ca/P proportion for HA tests is an essential parameter in determing its properties and thermal stability. The outcomes demonstrate obviously that HA stage was formed due to the Ca/P proportion which was kept up at 1.67.

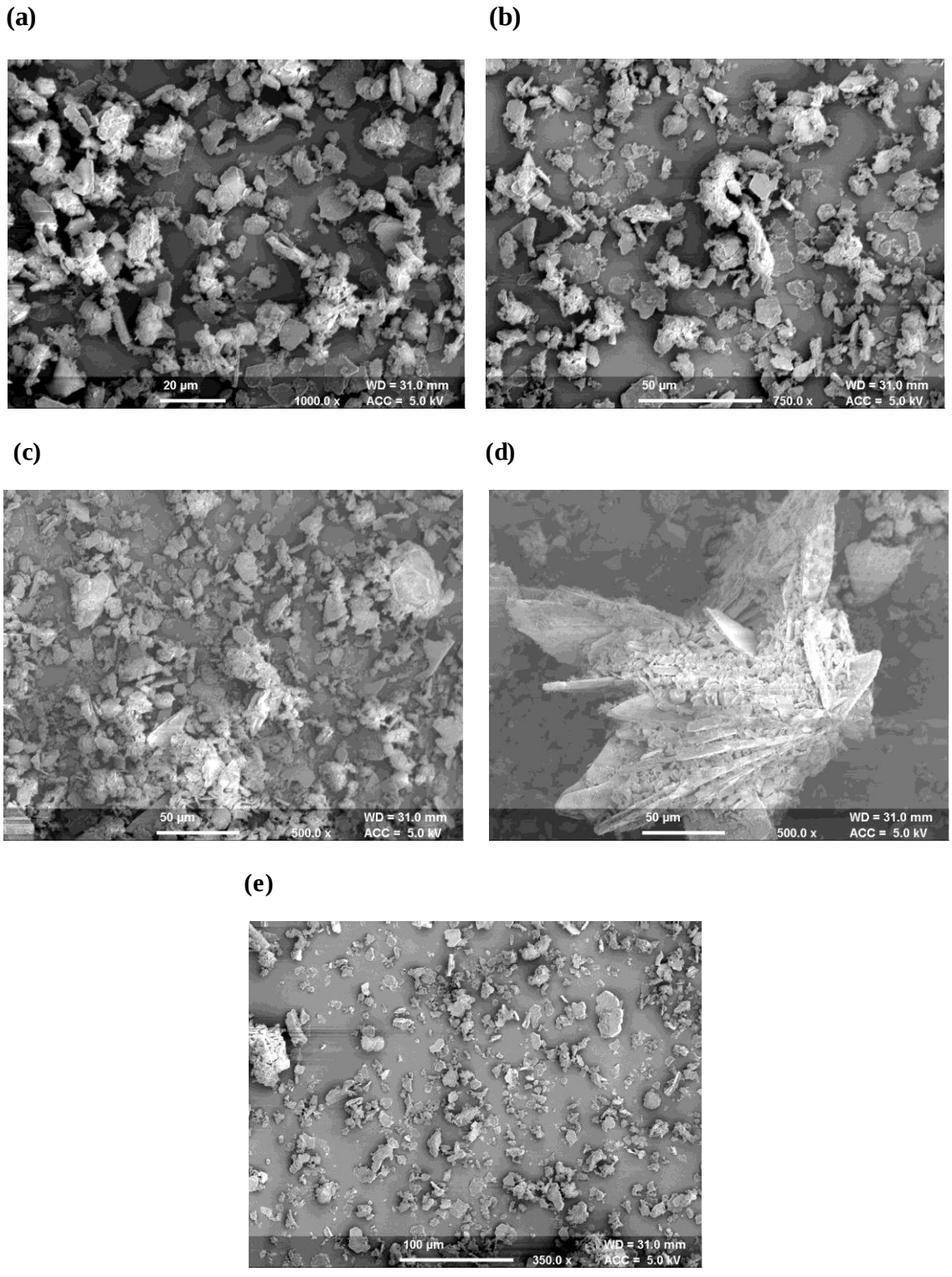

Figure 7.1.9: (a),(b),(c),(d) and (e) represents SEM images of HA formed from oyster shells

SEM ANALYSIS OF HA FTIR GRAPH PRODUCED FROM OYSTER SHELLS

The arrangement of the microstructures of HA in the sintering procedure can be ascribed to the propensity of particles to take shape and agglomerate at high temperatures. The particles had sporadic shapes, including little spheres, agglomerated together in a few sections. It can be inferred that higher temperature diminishes the likelihood of grain development and the densification can be improved.

7.2 HYDROXYAPATITE FROM EGG SHELLS

After the processing in furnace, the calcium oxide absorbs moisture and turns into calcium hydroxide and fine powder was made of it.

(a) **(b)**

Figure 7.2.1 : (a) and (b) represents egg shells after calcinations and powdering of egg shells using mortar and pestle

The amount of calcium hydroxide powder formed from those shells after calcination was weighed. The weight was noted.The weight that it displayed was 222.68 gram.

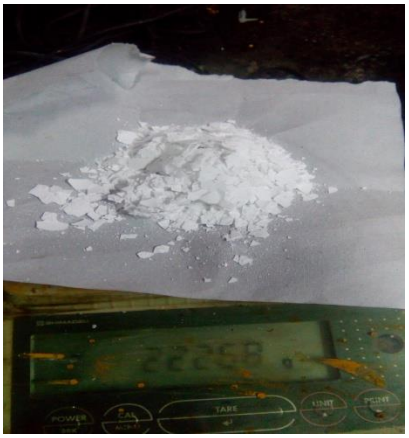

Figure 7.2.2 : represents weight of calcined egg shells

A small sample of it was given for FTIR analysis. FTIR is fourier transform Infrared Spectroscopy, where the infrared region of light is used to analyze the peaks of the bonds and stretch of the molecule.

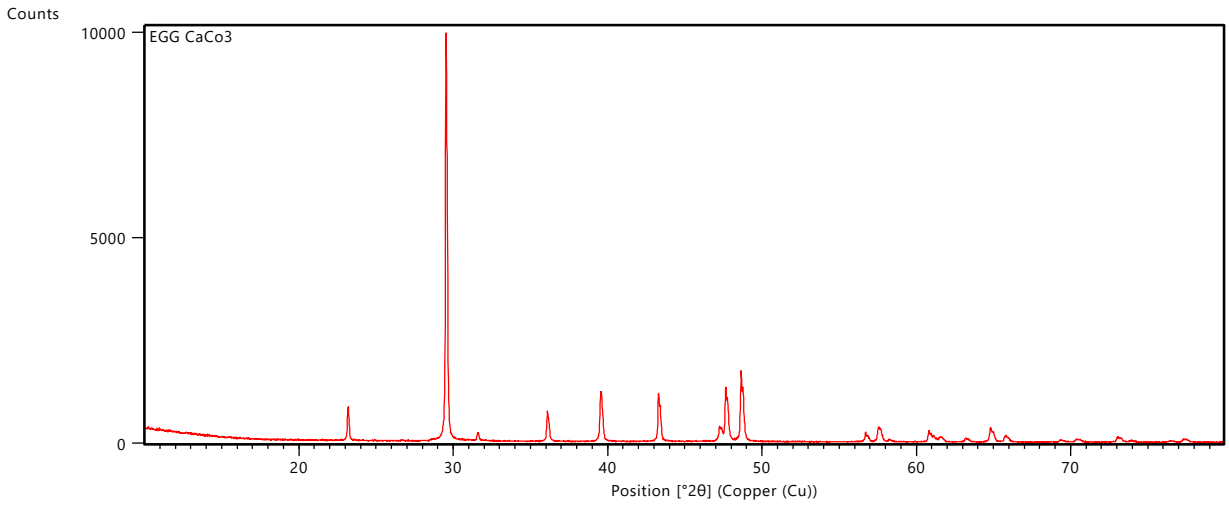

Figure 7.2.3: XRD of $CaCO_3$ formed from egg shells before processing

Dataset Name	EGG $CaCO_3$
File name	C:\XRD Data\APRIL l2017\EGG CaCo3.xrdml
Sample Identification	EGG CaCo3
Comment	Configuration=Reflection Spinner Stage, Owner=User-1, Creation date=20-09-2016 16:48:22

Goniometer=PW3050/60 (Theta/Theta); Minimum step size 2Theta:0.001; Minimum step size Omega:0.001

Sample stage=Spinner PW3064

Diffractometer system=XPERT-PRO

Measurement program=C:\PANalytical\Data Collector\Programs\Spinner.xrdmp, Identifier={544E0168-3858-47A1-AD8C-A5C91B0E4D3F}

Batch program=C:\PANalytical\Data Collector\Programs\SPINNER-1.xrdmp, Identifier={C20B4B02-C535-42F0-ADD7-4D3DF73E7C16}

PHD Lower Level = 6.52 (keV), PHD Upper Level = 12.80 (keV)

Measurement Start Date/Time	25-04-2017 11:57:50
Operator	User
Raw Data Origin	XRD measurement (*.XRDML)
Scan Axis	Gonio
Start Position [°2θ]	10.0084
End Position [°2θ]	79.9804
Step Size [°2θ]	0.0170
Scan Step Time [s]	29.8450
Scan Type	Continuous
PSD Mode	Scanning
PSD Length [°2θ]	2.12
Offset [°2θ]	0.0000
Divergence Slit Type	Fixed
Divergence Slit Size [°]	0.8709
Specimen Length [mm]	10.00
Measurement Temperature [°C]	25.00
Anode Material	Cu
K-Alpha1 [Å]	1.54060
Generator Settings	40 mA, 45 kV
Diffractometer Type	0000000011023505
Diffractometer Number	0
Goniometer Radius [mm]	240.00
Dist. Focus-Diverg. Slit [mm]	100.00
Incident Beam Monochromator	No

Spinning		Yes		
Pos. [°2θ]	FWHM Left [°2θ]	d-spacing [Å]	Rel. Int. [%]	Area [cts*°2θ]
23.1698	0.1171	3.83577	8.41	95.55
29.5289	0.1020	3.02261	100.00	1337.15
31.6299	0.1428	2.82646	1.97	36.91
36.0993	0.1020	2.48611	7.45	99.61
39.5348	0.1224	2.27763	11.35	182.19
43.2947	0.0816	2.08814	12.10	129.44
47.2471	0.0816	1.92226	3.71	39.72
47.6506	0.0816	1.90692	13.50	144.37
47.7850	0.0816	1.90187	10.26	109.73
48.6490	0.0816	1.87009	17.69	189.26
56.7111	0.0816	1.62188	2.45	26.19
57.5342	0.1224	1.60062	3.54	56.74
57.7058	0.1224	1.59627	3.15	50.58
58.2584	0.2448	1.58244	0.57	18.28
60.8199	0.1020	1.52178	2.80	37.48
61.6274	0.2448	1.50376	1.16	37.32
63.1917	0.1224	1.47025	0.89	14.29
64.8124	0.1428	1.43735	3.58	67.02
65.7634	0.2040	1.41884	1.42	37.88
69.3993	0.4080	1.35312	0.50	26.88
70.3701	0.1632	1.33682	0.70	14.92
73.0402	0.1632	1.29439	1.24	26.48
73.9329	0.4080	1.28096	0.34	18.22

76.4928	0.4080	1.24434	0.34	18.42
77.3792	0.4896	1.23228	0.72	46.01

XRD ANALYSIS OF CaCO3 OF EGG SHELLS BEFORE PROCESSING

From the XRD graph, the highest peak was observed at 2ɵ is 29.52^{o} where the relatively intensity was 100%. Calcium carbonate are the calcites. The sample analysis was done as such without any heat treatment to the CaCO3. The crystalline phase identified was JCPD, 5-0586.

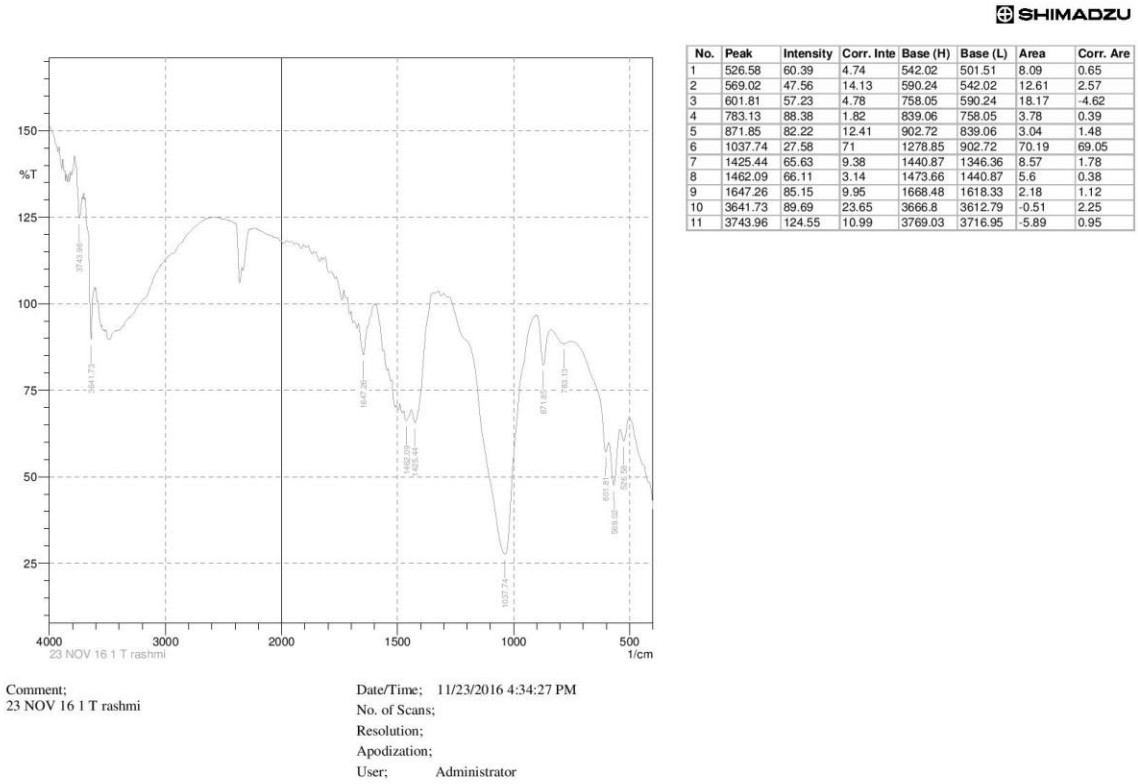

No.	Peak	Intensity	Corr. Inte	Base (H)	Base (L)	Area	Corr. Are
1	526.58	60.39	4.74	542.02	501.51	8.09	0.65
2	569.02	47.56	14.13	590.24	542.02	12.61	2.57
3	601.81	57.23	4.78	758.05	590.24	18.17	-4.62
4	783.13	88.38	1.82	839.06	758.05	3.78	0.39
5	871.85	82.22	12.41	902.72	839.06	3.04	1.48
6	1037.74	27.58	71	1278.85	902.72	70.19	69.05
7	1425.44	65.63	9.38	1440.87	1346.36	8.57	1.78
8	1462.09	66.11	3.14	1473.66	1440.87	5.6	0.38
9	1647.26	85.15	9.95	1668.48	1618.33	2.18	1.12
10	3641.73	89.69	23.65	3666.8	3612.79	-0.51	2.25
11	3743.96	124.55	10.99	3769.03	3716.95	-5.89	0.95

Figure 7.2.4 : FTIR of $Ca(OH)_2$ formed after processing (calcination) of egg shells

FTIR ANALYSIS OF $Ca(OH)_2$ PRODUCED FROM EGG SHELLS

Figure 7.2.3 represents that the calcium hydroxide produced from egg shells after calcinations at 800^oC was analyzed through FTIR. The graph resulted the presence of several peaks that is useful for studying the bending and stretching of the molecules present in it and also the type of functional group present in it. 526.58cm^{-1}, 569.02cm^{-1} and 601.81cm^{-1} wavenumber peak showed the presence of alkyl group whose intensity is very strong.783.13cm^{-1} wave number described the C-H bending whose intensity is also strong. 871.85cm^{-1} wave number revealed the presence of aromatic C-H bending. 1037.74cm^{-1} wave number peak told about the alkyl functional group whose intensity is strong. 1425.44cm^{-1}, 1462.09cm^{-1} wave number mentioned the presence of C-H bending which is aromatic in nature. 1647.26cm^{-1} wave number peak showed the presence of aromatic C=C bending and finally 3641.73cm^{-1} and 3743.96cm^{-1} showed the presence of amide N-H stretch [Silverstein, R.M *et al.*, 1981].

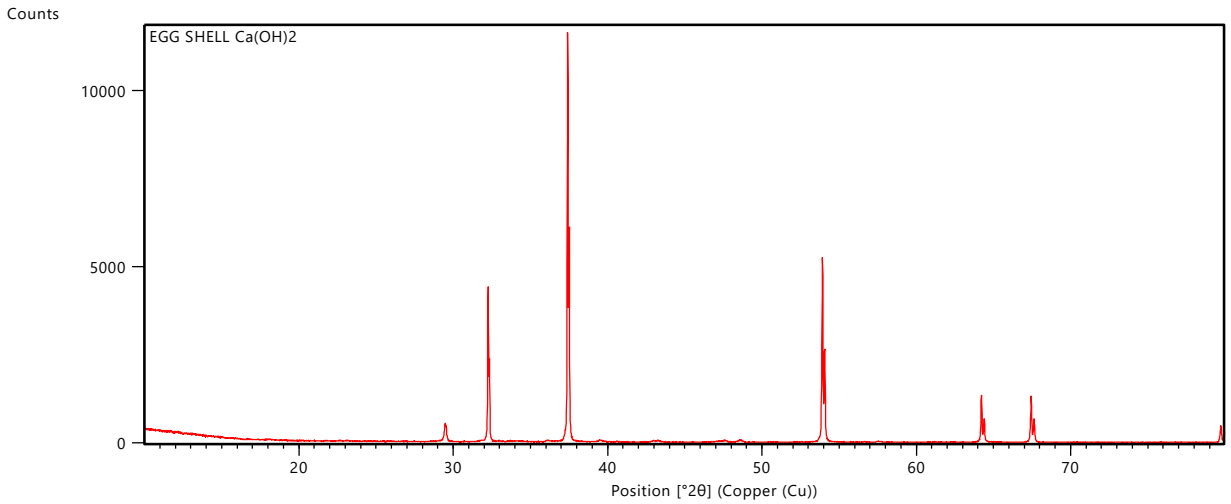

Figure 7.2.5: XRD of $Ca(OH)_2$ formed from egg shells

Dataset Name	EGG SHELL $Ca(OH)_2$
File name	C:\XRD Data\APRIL l2017\EGG SHELL Ca(OH)2.xrdml
Comment	Configuration=Reflection Spinner Stage, Owner=User-1, Creation date=20-09-2016 16:48:22

Goniometer=PW3050/60 (Theta/Theta); Minimum step size 2Theta:0.001; Minimum step size Omega:0.001

Sample stage=Spinner PW3064

Diffractometer system=XPERT-PRO

Measurement program=C:\PANalytical\Data Collector\Programs\Spinner.xrdmp, Identifier={544E0168-3858-47A1-AD8C-A5C91B0E4D3F}

PHD Lower Level = 6.52 (keV), PHD Upper Level = 12.80 (keV)

Measurement Start Date/Time	25-04-2017 14:37:40
Operator	User
Raw Data Origin	XRD measurement (*.XRDML)

Scan Axis	Gonio
Start Position [°2θ]	10.0084
End Position [°2θ]	79.9804
Step Size [°2θ]	0.0170
Scan Step Time [s]	29.8450
Scan Type	Continuous
PSD Mode	Scanning
PSD Length [°2θ]	2.12
Offset [°2θ]	0.0000
Divergence Slit Type	Fixed
Divergence Slit Size [°]	0.8709
Specimen Length [mm]	10.00
Measurement Temperature [°C]	25.00
Anode Material	Cu
K-Alpha1 [Å]	1.54060
Generator Settings	40 mA, 45 kV
Diffractometer Type	0000000011023505
Diffractometer Number	0
Goniometer Radius [mm]	240.00
Dist. Focus-Diverg. Slit [mm]	100.00
Incident Beam Monochromator	No
Spinning	Yes

Pos. [°2θ]	FWHM Left [°2θ]	d-spacing [Å]	Rel. Int. [%]	Area [cts*°2θ]
29.4493	0.0669	3.03060	4.48	34.72
32.2570	0.0612	2.77293	37.37	358.34
34.1971	0.6528	2.61992	0.21	21.71
36.1239	0.3264	2.48447	0.38	19.51
37.4109	0.0612	2.40190	100.00	958.95
39.5192	0.2040	2.27849	0.41	13.10
43.2987	0.2448	2.08795	0.37	14.16
47.6255	0.3264	1.90787	0.44	22.41
48.5744	0.2448	1.87279	0.53	20.16
50.8531	1.1424	1.79409	0.04	7.67
53.9209	0.0816	1.69903	45.52	582.01
57.5502	0.4080	1.60021	0.18	11.74
64.2204	0.0816	1.44916	11.57	147.96
67.4455	0.1020	1.38749	11.52	184.12
79.7359	0.1020	1.20168	3.96	63.36

XRD ANALYSIS OF Ca(OH)2 PRODUCED FROM EGG SHELLS

From the XRD pattern, it was observed that there were three high peaks formed at 2ɵ is 32.25^{o}, 37.41^{o} and 53.92^{o}. The relative intensity of the peaks were 37.37%, 100% and 45.52% respectively. The crystalline phase identified was JCPD, 4-0733.

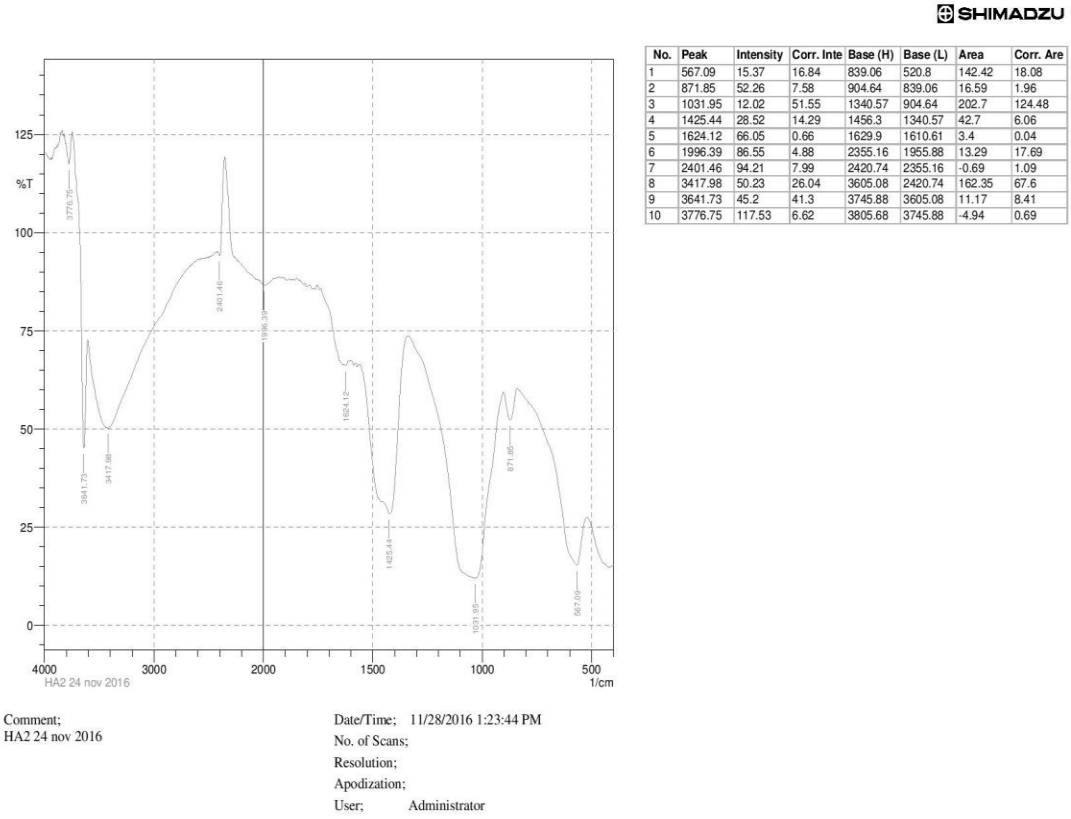

No.	Peak	Intensity	Corr. Inte	Base (H)	Base (L)	Area	Corr. Are
1	567.09	15.37	16.84	839.06	520.8	142.42	18.08
2	871.85	52.26	7.58	904.64	839.06	16.59	1.96
3	1031.95	12.02	51.55	1340.57	904.64	202.7	124.48
4	1425.44	28.52	14.29	1456.3	1340.57	42.7	6.06
5	1624.12	66.05	0.66	1629.9	1610.61	3.4	0.04
6	1996.39	86.55	4.88	2355.16	1955.88	13.29	17.69
7	2401.46	94.21	7.99	2420.74	2355.16	-0.69	1.09
8	3417.98	50.23	26.04	3605.08	2420.74	162.35	67.6
9	3641.73	45.2	41.3	3745.88	3605.08	11.17	8.41
10	3776.75	117.53	6.62	3805.68	3745.88	-4.94	0.69

Figure 7.2.6 : FTIR of HA formed from egg shells

FTIR ANALYSIS OF HA PRODUCED FROM EGG SHELLS

Figure 6.2.4 represents that the Hydroxyapatite produced by chemically treating the calcium hydroxide produced from egg shells was analyzed through FTIR. The report showed the peaks which revealed the presence of several functional groups with their bending and stretching properties. 567.09cm^{-1} wave number showed the presence of alkyl group. 871.85cm^{-1} wave number tells about the presence of aromatic C-H bending. 1031.95cm^{-1} wave number resulted in the presence of alkyl group whose intensity is strong. 1425.44cm^{-1} wave number described about the aromatic C-H bending.1624.12cm^{-1} and 1996.39cm^{-1} wave number stated the presence of C=C stretch. 2401.46cm^{-1}, 3417.98cm^{-1} wave number showed the presence of O-H stretch and also 3641.73cm^{-1} and 3776.75cm^{-1} resulted in the presence of O-H stretch.

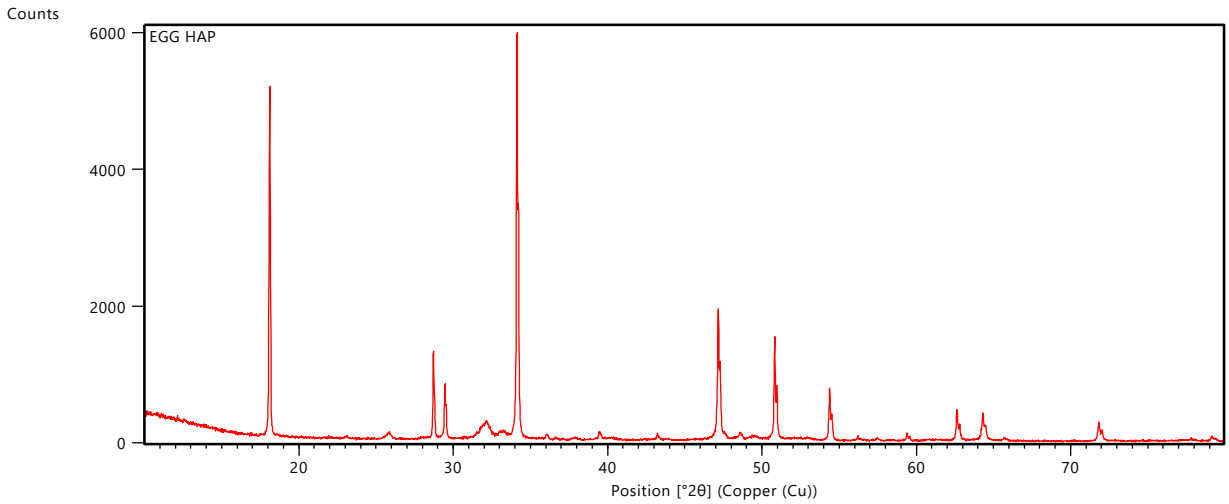

Figure 7.2.7: XRD of HA formed from egg shells

Dataset Name	EGG HAP
File name	C:\XRD Data\APRIL l2017\EGG HAP.xrdml
Sample Identification	EGG HAP
Comment	Configuration=Reflection Spinner Stage, Owner=User-1, Creation date=20-09-2016 16:48:22

Goniometer=PW3050/60 (Theta/Theta); Minimum step size 2Theta:0.001; Minimum step size Omega:0.001

Sample stage=Spinner PW3064

Diffractometer system=XPERT-PRO

Measurement program=C:\PANalytical\Data Collector\Programs\Spinner.xrdmp, Identifier={544E0168-3858-47A1-AD8C-A5C91B0E4D3F}

Batch program=C:\PANalytical\Data Collector\Programs\SPINNER-1.xrdmp, Identifier={C20B4B02-C535-42F0-ADD7-4D3DF73E7C16}

PHD Lower Level = 6.52 (keV), PHD Upper Level = 12.80 (keV)

Measurement Start Date/Time 25-04-2017 13:11:59

Operator	User
Raw Data Origin	XRD measurement (*.XRDML)
Scan Axis	Gonio
Start Position [°2θ]	10.0084
End Position [°2θ]	79.9804
Step Size [°2θ]	0.0170
Scan Step Time [s]	29.8450
Scan Type	Continuous
PSD Mode	Scanning
PSD Length [°2θ]	2.12
Offset [°2θ]	0.0000
Divergence Slit Type	Fixed
Divergence Slit Size [°]	0.8709
Specimen Length [mm]	10.00
Measurement Temperature [°C]	25.00
Anode Material	Cu
K-Alpha1 [Å]	1.54060
Generator Settings	40 mA, 45 kV
Diffractometer Type	0000000011023505
Diffractometer Number	0
Goniometer Radius [mm]	240.00
Dist. Focus-Diverg. Slit [mm]	100.00
Incident Beam Monochromator	No
Spinning	Yes

Pos. [°2θ]	FWHM Left [°2θ]	d-spacing [Å]	Rel. Int. [%]	Area [cts*°2θ]
18.0955	0.1004	4.89833	85.84	520.22
23.0825	0.2007	3.85009	0.46	5.55
25.8057	0.2342	3.44963	1.40	19.75
28.6885	0.0502	3.10922	21.41	64.86
29.4384	0.0669	3.03169	13.29	53.69
32.1547	0.2676	2.78151	4.26	68.78
34.1338	0.0816	2.62464	100.00	665.99
36.0554	0.2448	2.48904	1.26	25.20
36.6765	0.2448	2.44830	0.38	7.65
39.4698	0.2040	2.28123	1.78	29.61
43.2135	0.0816	2.09188	1.33	8.87
47.1728	0.0816	1.92511	31.93	212.63
48.5715	0.2040	1.87290	1.74	28.96
49.4723	0.4896	1.84088	0.89	35.48
50.8320	0.0816	1.79479	25.36	168.88
53.0656	0.4896	1.72438	0.52	20.78
54.3912	0.1020	1.68545	12.73	106.02
56.2093	0.1224	1.63516	0.90	8.98
57.5007	0.2448	1.60147	0.53	10.50
59.4001	0.0816	1.55472	1.90	12.64
62.6363	0.1020	1.48194	7.42	61.77
64.3341	0.1020	1.44687	6.28	52.28
65.7578	0.3264	1.41895	0.52	13.80

71.8343	0.1428	1.31313	4.71	54.91
77.6365	0.9792	1.22884	0.32	25.19
79.1497	0.1632	1.20910	1.11	14.75

XRD ANALYSIS OF HA PRODUCED FROM EGG SHELLS

From the XRD graph, two high intensity peaks located at 2ɵ is 18.09^{o} and 34.13^{o} were observed. The crystalline stages are distinguished are HAP JCPD, 9-0432., calcium oxide JCPD, 37-1497, calcium hydroxide JCPD, 4-0733. These outcomes can be clarified as an inadequate change of calcite, because of a temperature not sufficiently high or the consequences will be severe to the tempering time which is too short. HAP is by vast the fundamental crystalline stage phase. Besides, HAP is the unique apatite phase identified as a result of the procedure.

(a) **(b)**

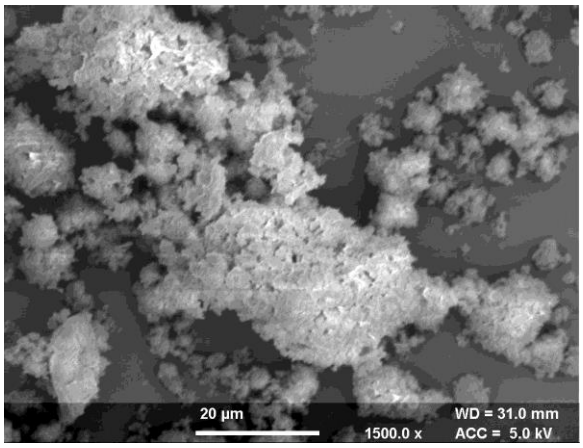

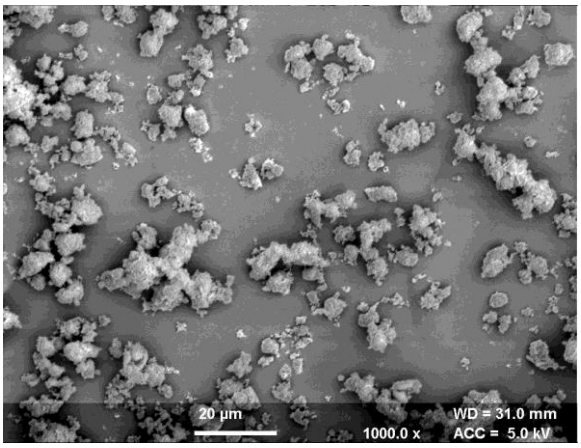

(c) (d)

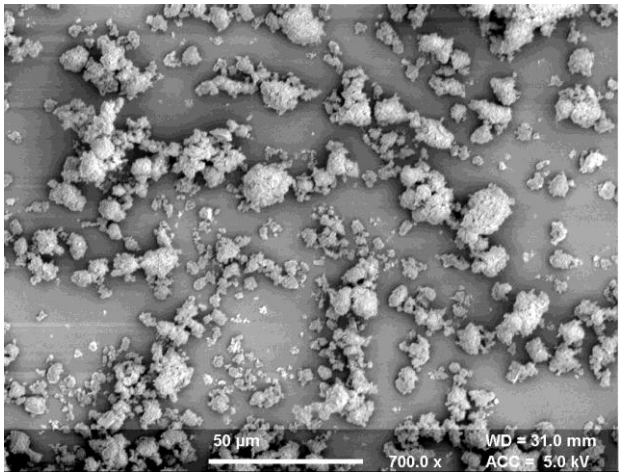

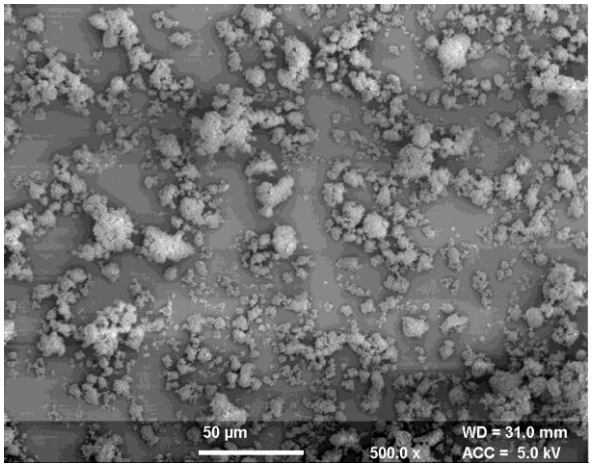

(e)

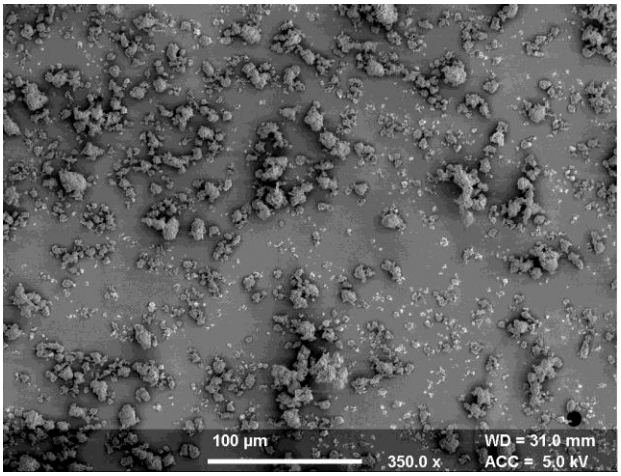

Figure 7.2.8: (a),(b),(c),(d) and (e) represents SEM images of HA formed from egg shells

SEM ANALYSIS OF HA PRODUCED FROM EGG SHELLS

After the thermal treatment, the morphologies of the material were observed. Irregular shaped agglomerates like morphology was observed and uniform pore size was visible. At different magnifications and measurements the observation was more clear and precise. SEM is one of the best technique to examine the morphology of the sample or material.

7.3 HYDROXYAPATITE FROM CRAB SHELLS

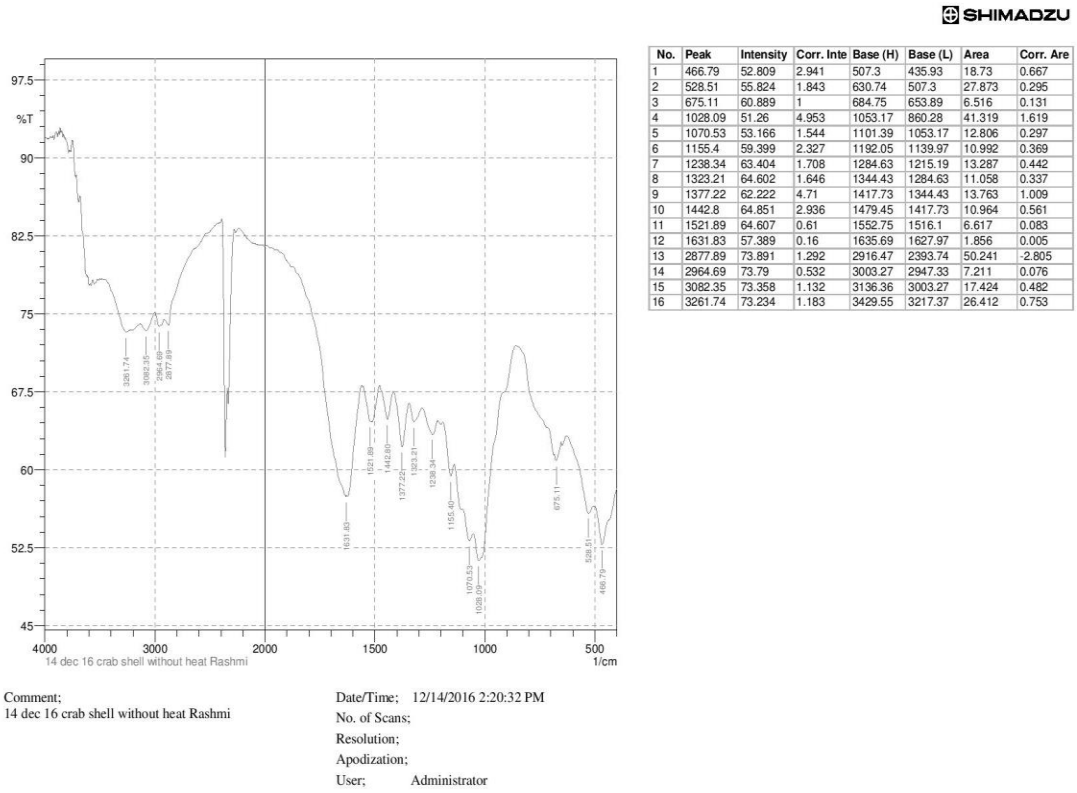

No.	Peak	Intensity	Corr. Inte	Base (H)	Base (L)	Area	Corr. Are
1	466.79	52.809	2.941	507.3	435.93	18.73	0.667
2	528.51	55.824	1.843	630.74	507.3	27.873	0.295
3	675.11	60.889	1	684.75	653.89	6.516	0.131
4	1028.09	51.26	4.953	1053.17	860.28	41.319	1.619
5	1070.53	53.166	1.544	1101.39	1053.17	12.806	0.297
6	1155.4	59.399	2.327	1192.05	1139.97	10.992	0.369
7	1238.34	63.404	1.708	1284.63	1215.19	13.287	0.442
8	1323.21	64.602	1.646	1344.43	1284.63	11.058	0.337
9	1377.22	62.222	4.71	1417.73	1344.43	13.763	1.009
10	1442.8	64.851	2.936	1479.45	1417.73	10.964	0.561
11	1521.89	64.607	0.61	1552.75	1516.1	6.617	0.083
12	1631.83	57.389	0.16	1635.69	1627.97	1.856	0.005
13	2877.89	73.891	1.292	2916.47	2393.74	50.241	-2.805
14	2964.69	73.79	0.532	3003.27	2947.33	7.211	0.076
15	3082.35	73.358	1.132	3136.36	3003.27	17.424	0.482
16	3261.74	73.234	1.183	3429.55	3217.37	26.412	0.753

Comment;
14 dec 16 crab shell without heat Rashmi

Date/Time; 12/14/2016 2:20:32 PM
No. of Scans;
Resolution;
Apodization;
User; Administrator

Figure 7.3.1 : FTIR of powdered crab shell before processing

FTIR ANALYSIS OF $CaCO_3$ OF CRAB SHELL BEFORE PROCESSING

Figure 7.3.1 represents that some small pieces of a crab shell were taken and washed, then kept sometime open to dry. The exoskeleton (crab shell) is nothing but calcium carbonate. The pieces were crushed and grinded to fine powder so that FTIR analysis can be done. The FTIR report revealed that the bands 528.51cm^{-1}, 1028.09cm^{-1}, 1070.53cm^{-1}, 1155.4cm^{-1}, 1377.22cm^{-1} showed alkyl halide functional group. The peak 675.1cm^{-1} showed C-H bending. The peaks 1238.34cm^{-1} and 1323.21cm^{-1} displayed amine C-N stretch. The wave number 1442.8cm^{-1} and 1521.89cm^{-1} showed aromatic C=C stretch. Peak 1631.83cm^{-1} revealed the presence of alkenyl C=C stretch. The peak 2877.89cm^{-1} resulted in the presence of alkyl C-H stretch. The peak 2964.69cm^{-1} showed carboxylic acid O-H stretch. Peak 3082.35cm^{-1} stated the presence of alkenyl C-H stretch. Finally wave number 3261.74cm^{-1} revealed the presence of O-H stretch [Silverstein, R.M *et al.*, 1981].

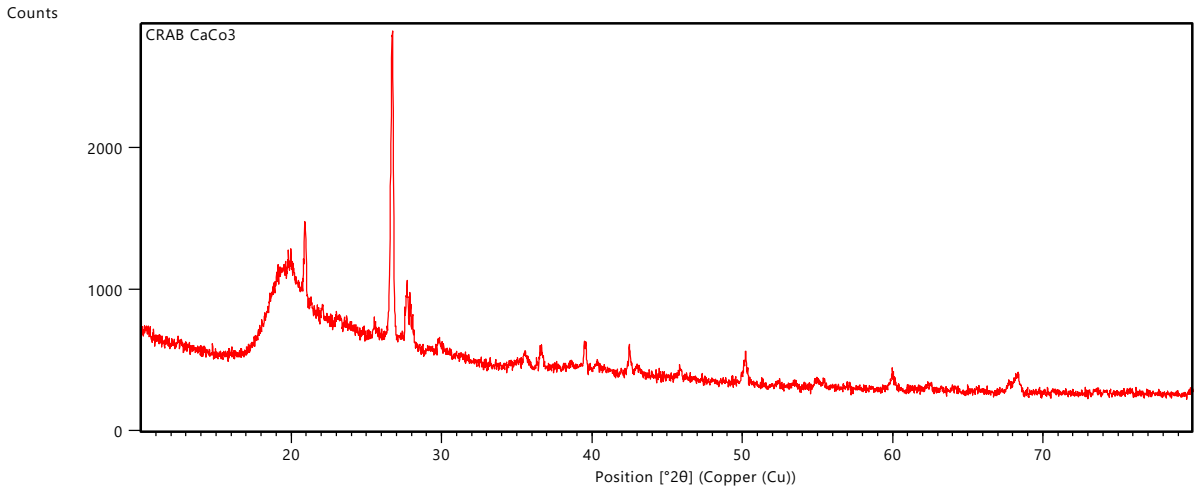

Figure 7.3.2: XRD of $CaCO_3$ formed from crab shells before processing

Dataset Name	CRAB $CaCO_3$
File name	C:\XRD Data\APRIL l2017\CRAB CaCo3.xrdml
Sample Identification	CRAB CaCo3
Comment	Configuration=Reflection Spinner Stage, Owner=User-1, Creation date=20-09-2016 16:48:22

Goniometer=PW3050/60 (Theta/Theta); Minimum step size 2Theta:0.001; Minimum step size Omega:0.001

Sample stage=Spinner PW3064

Diffractometer system=XPERT-PRO

Measurement program=C:\PANalytical\Data Collector\Programs\Spinner.xrdmp, Identifier={544E0168-3858-47A1-AD8C-A5C91B0E4D3F}

Batch program=C:\PANalytical\Data Collector\Programs\SPINNER-1.xrdmp, Identifier={C20B4B02-C535-42F0-ADD7-4D3DF73E7C16}

PHD Lower Level = 6.52 (keV), PHD Upper Level = 12.80 (keV)

Measurement Start Date/Time 25-04-2017 12:53:27

Operator	User
Raw Data Origin	XRD measurement (*.XRDML)
Scan Axis	Gonio
Start Position [°2θ]	10.0084
End Position [°2θ]	79.9804
Step Size [°2θ]	0.0170
Scan Step Time [s]	29.8450
Scan Type	Continuous
PSD Mode	Scanning
PSD Length [°2θ]	2.12
Offset [°2θ]	0.0000
Divergence Slit Type	Fixed
Divergence Slit Size [°]	0.8709
Specimen Length [mm]	10.00
Measurement Temperature [°C]	25.00
Anode Material	Cu
K-Alpha1 [Å]	1.54060
K-Alpha2 [Å]	1.54443
K-Beta [Å]	1.39225
K-A2 / K-A1 Ratio	0.50000
Generator Settings	40 mA, 45 kV
Diffractometer Type	0000000011023505
Diffractometer Number	0
Goniometer Radius [mm]	240.00
Dist. Focus-Diverg. Slit [mm]	100.00

Incident Beam Monochromator No

Pos. [°2θ]	FWHM Left [°2θ]	d-spacing [Å]	Rel. Int. [%]	Area [cts*°2θ]
19.2275	0.9368	4.61625	19.48	359.11
19.9676	0.5353	4.44678	22.56	237.63
20.9080	0.1338	4.24886	36.34	95.68
25.5539	0.2007	3.48594	4.81	18.99
26.7644	0.1506	3.33097	100.00	296.24
27.7074	0.1171	3.21970	23.56	54.29
27.8935	0.0502	3.19865	19.44	19.20
29.8480	0.2007	2.99350	4.34	17.15
35.6276	0.4015	2.52002	4.48	35.38
36.6189	0.2007	2.45405	6.76	26.69
39.5425	0.2007	2.27909	9.05	35.76
42.5102	0.1004	2.12660	9.62	19.00
45.8689	0.2007	1.97840	3.45	13.64
50.2255	0.1004	1.81653	11.45	22.62
54.9546	0.6691	1.67087	2.81	37.02
60.0291	0.2676	1.54120	5.20	27.39
62.4151	0.4015	1.48789	1.82	14.36
68.3095	0.4015	1.37317	6.18	48.85

XRD ANALYSIS OF $CaCO_3$ PRODUCED FROM CRAB SHELLS

From the XRD graph, three high peaks were observed at the location 2 ɵ was 20.9^o, 26.76^o and 27.70^o. The relative intensity observed was 36.34%, 100% and 23.56% respectively. The crystalline phase identified was JCPD, 5-0586.

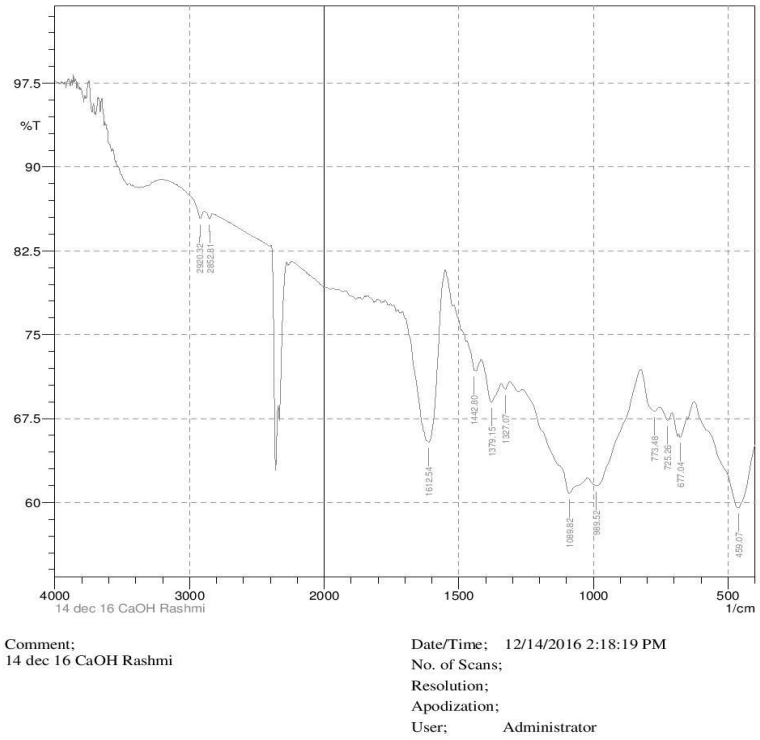

No.	Peak	Intensity	Corr. Inte	Base (H)	Base (L)	Area	Corr. Are
1	459.07	59.535	0.53	464.86	399.28	13.729	0.256
2	677.04	65.812	0.634	682.82	653.89	5.129	0.076
3	725.26	67.354	0.856	752.26	707.9	7.474	0.118
4	773.48	68.133	1.354	825.56	752.26	11.712	0.442
5	989.52	61.501	2.311	1022.31	825.56	36.408	2.03
6	1089.82	60.803	3.605	1263.42	1022.31	45.877	2.417
7	1327.07	70.12	0.598	1342.5	1309.71	4.989	0.056
8	1379.15	68.954	2.741	1417.73	1342.5	11.483	0.621
9	1442.8	71.776	0.378	1469.81	1438.94	4.199	0.005
10	1612.54	65.386	1.517	1618.33	1552.75	9.635	0.589
11	2852.81	85.372	0.524	2887.53	2831.6	3.748	0.06
12	2920.32	85.374	0.931	3068.85	2895.25	10.51	0.09

Figure 7.3.3 : FTIR of $Ca(OH)_2$ formed after processing (calcination) of crab shells

FTIR ANALYSIS OF $Ca(OH)_2$ PRODUCED FROM CRAB SHELLS

Figure 6.3.2 represents that the calcium hydroxide produced from egg shells after calcinations at 800^oC was analyzed through FTIR. The graph resulted the presence of several peaks that is useful for studying the bending and stretching of the molecules present in it and also the type of functional group present in it. The peaks 677.04cm^{-1}, 725.26cm^{-1} and 773.48cm^{-1} showed the presence of aromatic C-H bending. 989.52cm^{-1} wave number showed the presence of C-H bending. The peaks 1089.82cm^{-1} and 1327.07cm^{-1} stated the presence of alkyl group.1379.15cm^{-1} and 1442.8cm^{-1} resulted in the presence of C-H bending. Peak 1612.54cm^{-1} showed the presence of aromatic C=C bending. Finally peaks of wave number 2852.81cm^{-1} and 2920.32cm^{-1} stated the presence of alkyl C-H stretch [Silverstein, R.M *et al.*, 1981]

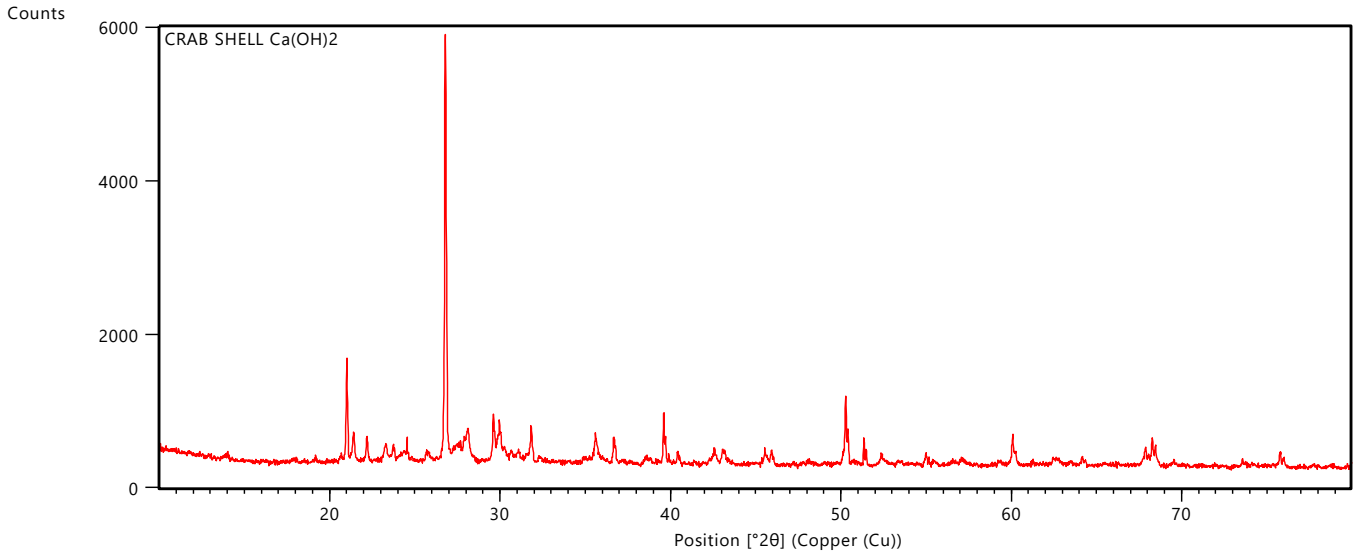

Figure 7.3.4: XRD of $Ca(OH)_2$ formed from crab shells

Dataset Name	CRAB SHELL $Ca(OH)_2$
File name	C:\XRD Data\APRIL l2017\CRAB SHELL Ca(OH)2.xrdml
Sample Identification	CRAB SHELL Ca(OH)2
Comment	Configuration=Reflection Spinner Stage, Owner=User-1, Creation date=20-09-2016 16:48:22

Goniometer=PW3050/60 (Theta/Theta); Minimum step size 2Theta:0.001; Minimum step size Omega:0.001

Sample stage=Spinner PW3064

Diffractometer system=XPERT-PRO

Measurement program=C:\PANalytical\Data Collector\Programs\Spinner.xrdmp, Identifier={544E0168-3858-47A1-AD8C-A5C91B0E4D3F}

Batch program=C:\PANalytical\Data Collector\Programs\SPINNER-1.xrdmp, Identifier={C20B4B02-C535-42F0-ADD7-4D3DF73E7C16}

PHD Lower Level = 6.52 (keV), PHD Upper Level = 12.80 (keV)

Measurement Start Date/Time	25-04-2017 12:34:54
Operator	User
Raw Data Origin	XRD measurement (*.XRDML)
Scan Axis	Gonio
Start Position [°2θ]	10.0084
End Position [°2θ]	79.9804
Step Size [°2θ]	0.0170
Scan Step Time [s]	29.8450
Scan Type	Continuous
PSD Mode	Scanning
PSD Length [°2θ]	2.12
Offset [°2θ]	0.0000
Divergence Slit Type	Fixed
Divergence Slit Size [°]	0.8709
Specimen Length [mm]	10.00
Measurement Temperature [°C]	25.00
Anode Material	Cu
K-Alpha1 [Å]	1.54060
Generator Settings	40 mA, 45 kV
Diffractometer Type	0000000011023505
Diffractometer Number	0
Goniometer Radius [mm]	240.00
Dist. Focus-Diverg. Slit [mm]	100.00

Incident Beam Monochromator No

Spinning Yes

Main Graphics, Analyze View:

Peak List:

Pos. [°2θ]	FWHM Left [°2θ]	d-spacing [Å]	Rel. Int. [%]	Area [cts*°2θ]
13.9565	0.2007	6.34031	1.25	14.14
20.9932	0.0836	4.22830	24.49	115.21
21.4182	0.1171	4.14534	6.47	42.62
22.1681	0.1004	4.00679	5.72	32.28
23.2936	0.1673	3.81567	4.26	40.13
23.7356	0.1004	3.74560	3.63	20.51
24.5278	0.0502	3.62639	5.90	16.65
25.6633	0.1338	3.46846	2.41	18.14
26.7658	0.1004	3.32803	100.00	564.58
28.0959	0.1338	3.17343	7.58	57.04
29.5865	0.0502	3.01685	11.18	31.55
29.9736	0.1338	2.97877	7.61	57.25
31.8010	0.0669	2.81165	8.26	31.09
32.3138	0.2007	2.76819	1.18	13.34
35.5758	0.1338	2.52148	5.97	44.96
36.6541	0.0669	2.44975	6.18	23.25
38.5170	0.3346	2.33544	1.50	28.17
39.5759	0.0502	2.27535	12.28	34.68
39.8721	0.0502	2.25913	2.60	7.34

40.4031	0.1004	2.23066	2.84	16.03
42.5515	0.1338	2.12287	3.95	29.75
43.0255	0.1338	2.10058	3.45	25.94
45.5059	0.1004	1.99168	3.26	18.43
45.8810	0.1338	1.97627	3.08	23.17
48.1427	0.5353	1.88857	0.76	22.80
50.2828	0.0816	1.81309	16.15	100.21
51.3520	0.0612	1.77782	6.38	29.69
52.3863	0.1224	1.74513	2.64	24.61
54.9950	0.1224	1.66836	2.73	25.38
57.1399	0.2448	1.61072	1.68	31.36
60.0907	0.0816	1.53849	7.38	45.80
62.5495	0.4896	1.48379	1.54	57.48
64.2275	0.3264	1.44902	1.28	31.87
67.8924	0.1020	1.37944	4.25	32.97
68.2789	0.0816	1.37257	6.55	40.65
69.5433	0.3264	1.35067	0.97	23.97
73.6482	0.4896	1.28520	1.06	39.50
75.7974	0.1224	1.25401	3.03	28.22

XRD ANALYSIS OF $Ca(OH)_2$ PRODUCED FROM CRAB SHELLS

From the XRD graph, two high peaks were observed at 2 ɵ was 29.99^o and 26.76^o. The relative intensity observed was 29.49% and 100% respectively. The crystalline phase identified was JCPD, 4-0733.

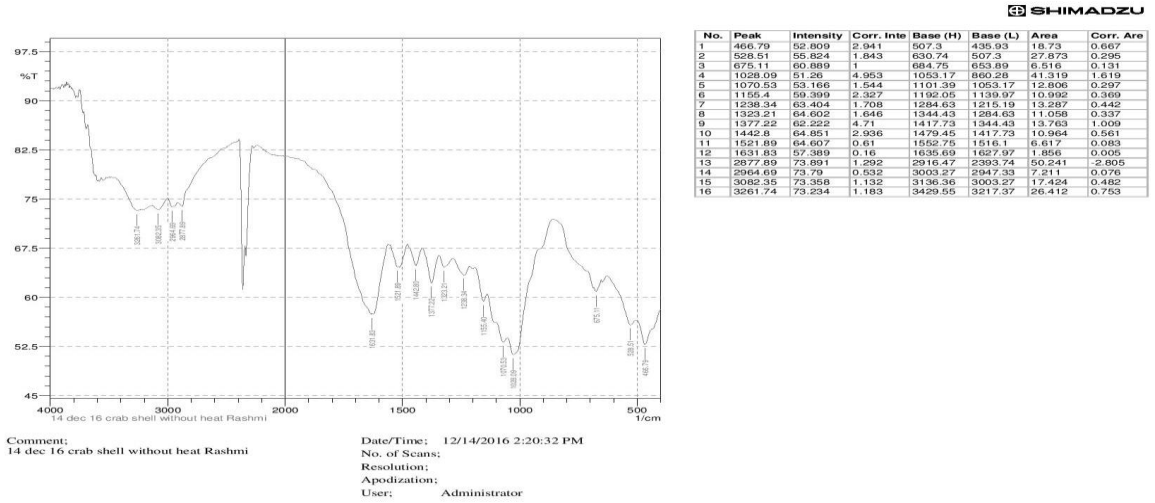

No.	Peak	Intensity	Corr. Inte	Base (H)	Base (L)	Area	Corr. Are
1	466.79	52.809	2.941	507.3	435.93	18.73	0.667
2	528.51	55.824	1.843	630.74	507.3	27.873	0.295
3	675.11	60.889	1	684.75	653.89	6.516	0.131
4	1028.09	51.26	4.953	1053.17	860.28	41.319	1.619
5	1070.53	53.166	1.544	1101.39	1053.17	12.806	0.297
6	1155.4	59.399	2.327	1192.05	1139.97	10.992	0.369
7	1238.34	63.404	1.708	1284.63	1215.19	13.287	0.442
8	1323.21	64.602	1.646	1344.43	1284.63	11.058	0.337
9	1377.22	62.222	4.71	1417.73	1344.43	13.763	1.009
10	1442.8	64.851	2.936	1479.45	1417.73	10.964	0.561
11	1521.89	64.607	0.61	1552.75	1516.1	6.617	0.083
12	1631.83	57.389	0.16	1635.69	1627.97	1.856	0.005
13	2877.89	73.891	1.292	2916.47	2393.74	50.241	2.805
14	2964.69	73.79	0.532	3003.27	2947.33	7.211	0.076
15	3082.35	73.358	1.132	3136.36	3003.27	17.424	0.482
16	3261.74	73.234	1.183	3429.55	3217.37	26.412	0.753

Figure 7.3.5: FTIR of HA formed from crab shells

represents that the calcium hydroxide produced from egg shells after calcinations at 800^{o}C was analyzed through FTIR. The graph resulted the presence of several peaks that is useful for studying the bending and stretching of the molecules present in it and also the type of functional group present in it. The peaks 677.04cm^{-1}, 725.26cm^{-1} and 801.27cm^{-1} showed the presence of aromatic C-H bending. 989.52cm^{-1} wave number showed the presence of C-H bending. The peaks 1089.82cm^{-1} and 1327.07cm^{-1} stated the presence of alkyl group.1379.15cm^{-1} and 1442.8cm^{-1} resulted in the presence of C-H bending. Peak 1612.54cm^{-1} showed the presence of aromatic C=C bending. Finally peaks of wave number 2852.81cm^{-1} and 3560.12cm^{-1} stated the presence of alkyl O-H stretch [Silverstein, R.M *et al.*, 1981]

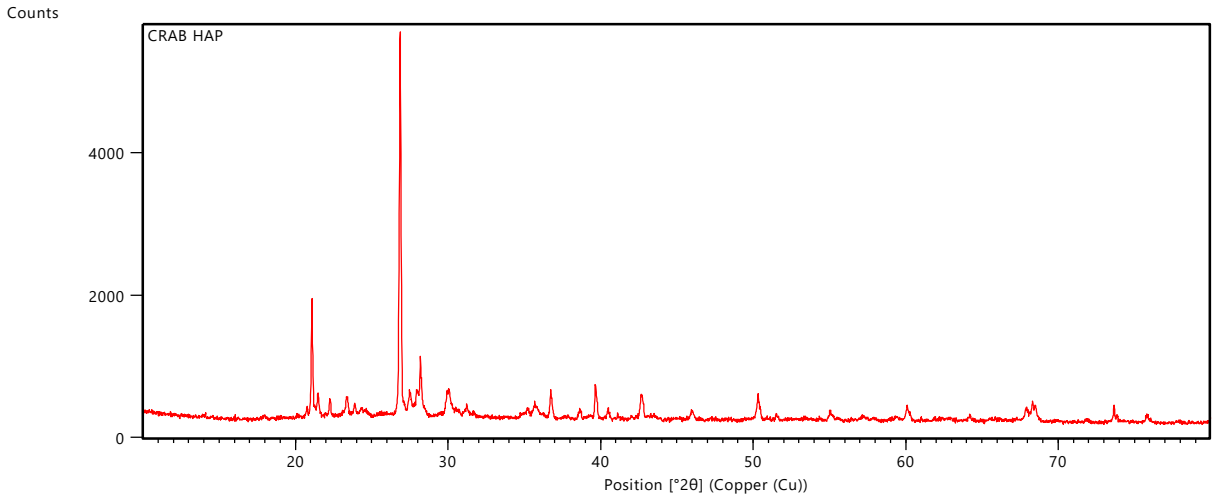

Figure 7.3.6: XRD of HA formed from crab shells

Dataset Name	CRAB HAP
File name	C:\XRD Data\APRIL l2017\CRAB HAP.xrdml
Sample Identification	CRAB HAP
Comment	Configuration=Reflection Spinner Stage, Owner=User-1, Creation date=20-09-2016 16:48:22

Goniometer=PW3050/60 (Theta/Theta); Minimum step size 2Theta:0.001; Minimum step size Omega:0.001

Sample stage=Spinner PW3064

Diffractometer system=XPERT-PRO

Measurement program=C:\PANalytical\Data Collector\Programs\Spinner.xrdmp, Identifier={544E0168-3858-47A1-AD8C-A5C91B0E4D3F}

Batch program=C:\PANalytical\Data Collector\Programs\SPINNER-1.xrdmp, Identifier={C20B4B02-C535-42F0-ADD7-4D3DF73E7C16}

PHD Lower Level = 6.52 (keV), PHD Upper Level = 12.80 (keV)

Measurement Start Date/Time	25-04-2017 12:16:22
Operator	User
Raw Data Origin	XRD measurement (*.XRDML)
Scan Axis	Gonio
Start Position [°2θ]	10.0084
End Position [°2θ]	79.9804
Step Size [°2θ]	0.0170
Scan Step Time [s]	29.8450
Scan Type	Continuous
PSD Mode	Scanning
PSD Length [°2θ]	2.12
Offset [°2θ]	0.0000
Divergence Slit Type	Fixed
Divergence Slit Size [°]	0.8709
Specimen Length [mm]	10.00
Measurement Temperature [°C]	25.00
Anode Material	Cu
K-Alpha1 [Å]	1.54060
K-Alpha2 [Å]	1.54443
K-Beta [Å]	1.39225
K-A2 / K-A1 Ratio	0.50000
Generator Settings	40 mA, 45 kV
Diffractometer Type	0000000011023505
Diffractometer Number	0
Goniometer Radius [mm]	240.00

Dist. Focus-Diverg. Slit [mm]	100.00
Incident Beam Monochromator	No
Spinning	Yes

Peak List:

Pos. [°2θ]	FWHM Left [°2θ]	d-spacing [Å]	Rel. Int. [%]	Area [cts*°2θ]
20.7529	0.1004	4.28026	2.28	12.43
21.0800	0.1004	4.21456	31.55	172.34
21.4801	0.0836	4.13696	6.38	29.05
22.2523	0.0836	3.99512	4.98	22.65
23.3881	0.1338	3.80362	5.18	37.70
23.8947	0.1338	3.72411	3.27	23.81
26.8621	0.1171	3.31906	100.00	637.26
27.5128	0.1673	3.24203	6.41	58.33
28.1846	0.0502	3.16627	15.63	42.68
30.0826	0.2676	2.97068	6.95	101.22
31.2215	0.2676	2.86487	2.51	36.55
35.7092	0.2676	2.51445	3.37	49.02
36.7232	0.0669	2.44732	6.75	24.59
38.6880	0.2007	2.32744	2.12	23.20
39.6591	0.0836	2.27265	8.99	40.93
40.4792	0.1338	2.22849	2.39	17.38
42.6810	0.2007	2.11848	6.19	67.61
45.9786	0.2007	1.97393	2.42	26.46
50.3229	0.0669	1.81324	6.99	25.47

51.5563	0.2007	1.77273	1.20	13.15
55.0493	0.1004	1.66823	2.59	14.14
57.4576	0.8029	1.60390	0.62	27.14
60.0958	0.1338	1.53965	3.58	26.06
62.5416	0.8029	1.48519	0.49	21.40
64.1775	0.2007	1.45122	1.13	12.29
67.8989	0.1338	1.38047	3.27	23.82
68.4116	0.3346	1.37137	3.46	63.06
73.6629	0.0612	1.28498	4.60	20.71
75.7921	0.1673	1.25513	1.64	14.96

XRD ANALYSIS OF HA PRODUCED FROM CRAB SHELLS

From the XRD graph, two high intensity peaks located at 2ɵ is 21.08^{o} and 26.86^{o} were observed. The diffractograms of sintering outcomes shows that the temperature is firmly identified with the arrangement of crystals. This is because of the way of the vibrating particles moving quicker in higher temperatures. The ideal temperature arrangement of hydroxyapatite was controlled by figuring of the likelihood of the test phase from the XRD comes about investigation agreeing to JCPDS standard information, which, JCPDS; 24-0033 is standard information for HAP; 09-0169 for beta-tri calcium phosphate; 29-0359 for alpha tricalcium phosphate.

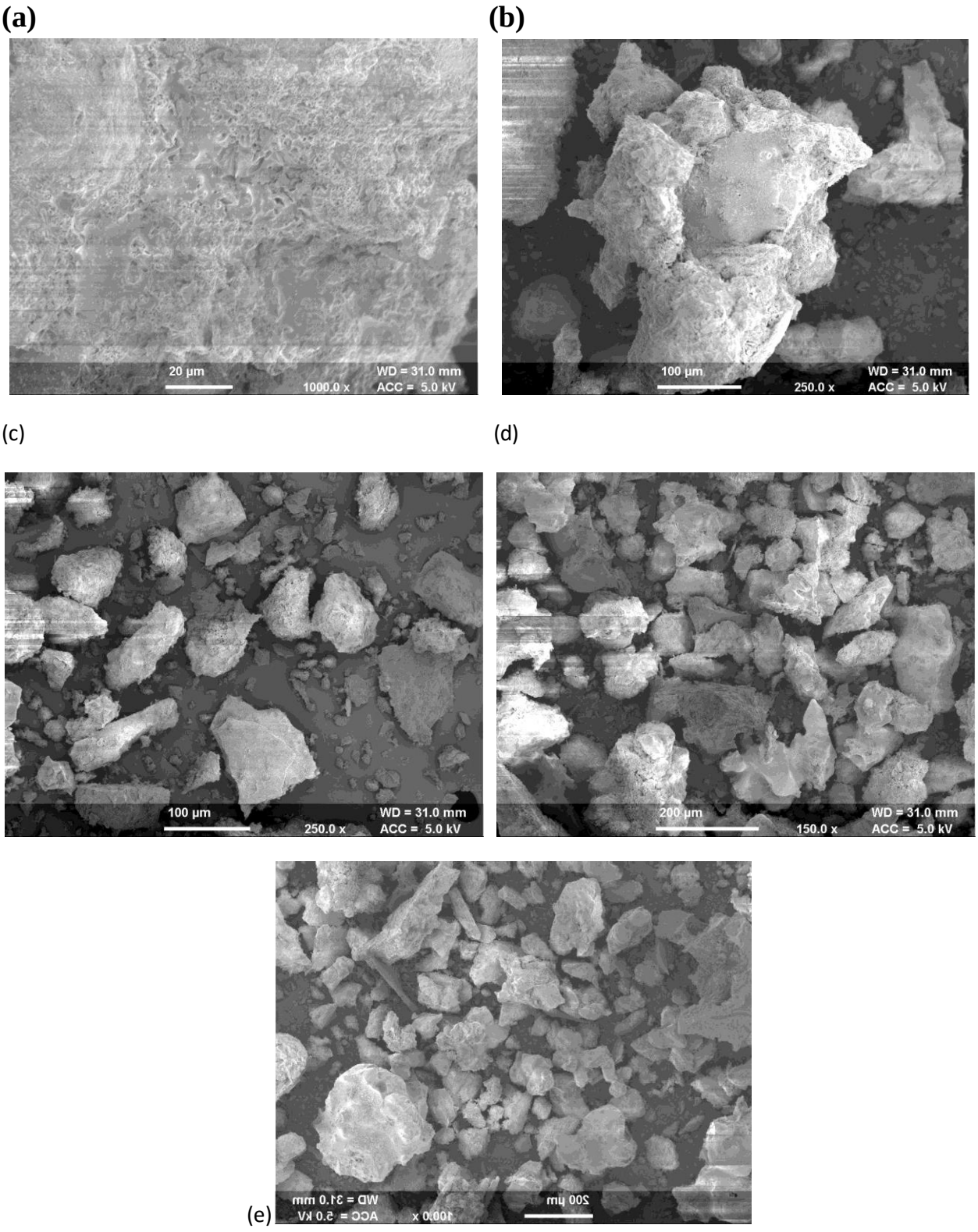

Figure 7.3.7: (a),(b),(c),(d) and (e) represents SEM images of HA formed from crab shells

SEM ANALYSIS OF HA PRODUCED FROM CRAB SHELLS

The SEM micrographs shows that the size of hydroxyapatite formed from the synthesis tends to be small and only a few are large.shows that the surface of hydroxyapatite is smooth and nonporous, this shows that hydroxyapatite which has synthesis from crab shells can function well as inhibiting tooth demineralization. The proportions of oxygen, calcium and phosphorus in the composition confirmed the composition of hydroxyapatite. It can be concluded that the synthesis results can be achieved to target.

Comparing HAP produced from oyster shells, egg shells and crab shells where the ground of comparison is FTIR, XRD and SEM :

The standard FTIR of hydroxyapatite have two major areas of discussion which can be a reference to compare HAP produced from other sources are O-H stretching band produced at the wave length 3575^{-1} and weak band of CO_3^{2-} produced at the wavelength 834.65^{-1}. Now with reference to this, HAP produced from oyster shells has O-H bending stretch at 2393.74^{-1} and 3408.33^{-1} and weak band of CO_3^{2-} at 873.78^{-1}. HAP produced from egg shells has O-H bending stretch at $3417.98^{-1}$and weak band of CO_3^{2-} at 871.85^{-1}. HAP produced from crab shells has O-H stretching band at 3560.12^{-1} and weak band of CO_3^{2-} at 801.27^{-1}. So, in the FTIR analysis HAP produced from crab shells showed similarity wave length with the standard HAP.

The standard XRD of hydroxyapatite can be compared to other HAP produced from different sources by means of JCPDS (Joint Committee on Powder Diffraction Strandards). Other major areas of discussion which are pos.2ɵ and relative intensity. The pos.2ɵ for 100% relative intensity of standard HAP is 26^{o}.The relative intensity is 100% for HAP produced from oyster shells is at 18.1^{o}, from egg shells is 34.13^{o} and from crab shells is 26.76^{o}. The standard JCPDS of hydroxyapatite is 9-0432 which was similar to HAP produced from crab shells.

The standard SEM analysis of hydroxyapatite is based on its morphological characters. Spherical and agglomerated morphology showed by standard HAP can be made as a reference to compare with other HAP produced from different sources. HAP produced from crab shells showed the similar morphological features as of standard HAP.

Hence from the above comparative analysis, it is clear that the hydroxyapatite produced from the crab shells is more qualitative than HAP produced from oyster and egg shells.

CHAPTER-8

CONCLUSION AND FUTURE SCOPE

CONCLUSION

As hydroxyapatite is an important constituent of teeth and bone so many research work are being conducted for its synthesis and implementation in real life medical use.

Basically, in this project the synthesis of hydroxyapatite was carried out by using naturally occuring waste calcium carbonate sources such as oyster shells, egg shells and crab shells. By several operations and treatments finally hydroxyapatite synthesis was done. This included calcination of calcium carbonate which is otherwise termed as calcination. The temperature required was high. It was set to 800^{o}C; which in turn converted the calcium carbonate into calcium oxide. Calcium oxide ($CaCO_3$) when absorbs moisture it got converted into calcium hydroxide ($Ca(OH)_2$). When calcium hydroxide is treated with orthophosphoric acid (H_3PO_4) it produced hydroxyapatite ($Ca_5(PO_4)_6(OH)_2$) and water (H_2O). It worked by a general phenomena i.e when base and acid reacts it gives rise to salt and water. In the same way the HA synthesis was done.

For the analysis of calcium hydroxide and hydroxyapatite FTIR was done. So depending upon the molecular behavior in the infrared region the peaks that were obtained was generally used to know which functional group is present and what are the bending and stretching characteristics of the matter.

From the above FTIR, SEM, XRD analysis it was clear that the HA synthesized was pure white hydroxyapatite.

FUTURE SCOPE

Hydroxyapatite (HAp) is a calcium phosphate like the human hard tissues in morphology and composition1. Especially, it has a hexagonal structure and a stoichiometric Ca/P proportion of 1.67, which is indistinguishable to bone apatite.

An imperative normal for hydroxyapatite is its soundness when contrasted with other calcium phosphates. Thermodynamically, hydroxyapatite is the most stable calcium phosphate compound under physiological conditions as temperature, pH and organization of the body fluids2.

With the advancement of nanotechnology, a noteworthy effect on materials science has been taken note. The creation of nanomaterials has increased extensive consideration for adsorption, catalysis and optical applications, especially when biomaterials are involved.

- Some remarkable properties of hydroxyapatite are:

- Biocompatibility
- Bioactivity
- Osteoconductivity
- Non danger and non incendiary nature

- The hydroxyapatite bioceramic has an assortment of uses that include:

- Bone tissue designing
- Bone void fillers for orthopedic, traumatology, spine, maxillofacial and dental surgery.
- Orthopedic and dental embed covering
- Reclamation of periodontal imperfections
- Edentulous edge expansion
- Endodontic treatment like mash topping
- Repair of mechanical furcation holes and apical obstruction arrangement
- Fillers for strengthening therapeutic glass ionomer bond (GIC) and helpful composite sap
- Desensitizing specialist in post teeth fading
- Remineralizing specialist in toothpastes

As these were the various reasons that makes the importance of synthesis of hydroxyapatite at its peak to study its properties as well as its usage in biomedical application.

CHAPTER-9
REFERENCES

REFERENCES

1. A.R. Kmita, A. Slosarczyk, Z. Paszkiewicz and C. Paluszkiewicz, “Phase stability of hydroxyapatite-zirconia (HAp – ZrO2) composites for bone replacement”, Journal of molecular structure, 704, 333-340 (2004).

2. Afshar, M. Ghorbani, N. Ehsani, M.R. Saeri and C.C. Sorrell, “Some important factors in the wet precipitation process of hydroxyapatite”, Materials and Design, 24, 197-202 (2003).
.

3. C.G. Vazquez, C.P. Barba and N. Munguia, “Stoichiometric hydroxyapatite obtained by precipitation and sol gel processes”, Revista Mexicana De Fisica, 51**,** 3, 284–293 (2005).

4. C.L. Yun, Z.C. Bo and H.J. Feng, “Influence of temperature, [Ca2+], Ca/P ratio and ultrasonic power on the crystallinity and morphology of hydroxyapatite nano particles prepared with a novel ultrasonic precipitation method, Materials Letters, 59, 1902-1906 (2005).

5. D. C. Tancred, A. J. Carr, B. A. O. McCormack, “The sintering and mechanical behavior of hydroxyapatite with bioglass additions”, Journal of Materials Science: Materials in Medicine, 12**,** 81–93 (2001).

6. D. Choi and P.N. Kumta, “An alternate chemical route for the synthesis and thermal stability of chemically enriched hydroxyapatite”, J. Am. Ceram. Soc., 89, 444-449 (2006).

7. D. J. Curran, T. J. Fleming, M.R. Towler, S. Hampshire, “Mechanical properties of hydroxyapatite-zirconia compacts sintered by two different sintering methods”, J. Mater Sci.: Mater Med, 21, 1109-1120 (2009)

8. Delgado, S. Martinez, L. Morejon, M.P. Ginebra, E. Fernandez, M.T. Clavaguera- Mora, J.R. Viejo, F.J. Gil and J.A. Planell, “Physical and mechanical behaviour of zirconia - hydroxyapatite ceramics after aging in simulated body fluid”, Key Engineering Materials, 218-220, 161-164 (2002).

9. E.S. Ahn, N.J. Gleason and J.Y. Ying, “The effect of zirconia reinforcing agents on the microstructure and mechanical properties of hydroxyapatite - based nanocomposites”,J. Am. Ceram. Soc, 88, 3374-3379 (2005).

10. F.N. Oktar and G. Goller, “Sintering effects on mechanical properties of glass reinforced hydroxyapatite composites”, Ceramic International, 28, 617-621(2002).

11. F.N. Oktar and G. Goller, “Sintering effects on mechanical properties of glass reinforced hydroxyapatite composites”, Ceramic International, 28, 617-621(2002).

12. H. Varma, S.P. Vijayan and S.S. Babu, “Transparent hydroxyapatite ceramics through gel casting and low temperature sintering”, J. Am. Ceram. Soc, 85, 493-495 (2002).

13. H. W. Kim, Y. H. Koh, B. H. Yoon, and H. E. Kim, “Reaction sintering and mechanical properties of hydroxyapatite-zirconia composites with calcium fluoride additions“, J.Am. Ceram. Soc., 85, 634 (2002).

14. H. W. Kim, Y. H. Koh, B. H. Yoon, and H. E. Kim, “Reaction sintering and mechanical properties of hydroxyapatite-zirconia composites with calcium fluoride additions“, J.Am. Ceram. Soc., 85, 634 (2002).

15. K. Donadel and M.C.M. Laranjeira, V.L. Gonealves, V.T. Faver, J.C. Lima and L.H.M. Prates, “Hydroxyapatite produced by wet- chemical methods”, J. Am. Ceram. Soc., 88, 2230-2245 (2005).

16. K.H. Prakash, C.P. Ooi, R. Kumar, K.A. Khor, P. Cheang, "Effect of super saturation level on the size and morphology of hydroxyapatite precipitate", IEEE, (2006).
17. L. B. Kong, J. Ma and F. Boey, "Nanosized hydroxyapatite powders derived from Co precipitation process", Journal of Materials Science 37, 1131(2002).
18. M.R. Saeri, A. Afshar, M. Ghorbani, N. Ehsani and C.C. Sorrell, "Wet precipation process of hydroxyapatite", Materials letter, 57, 4064-4069 (2003).
19. M.S. Abu Bakar, P. Cheang and K.A. Khor, Mater. Sci. Eng. A, 345, 55 (2003).
20. M.S. Abu Bakar, P. Cheang and K.A. Khor, Mater. Sci. Eng. A, 345, 55 (2003).
21. Mobasherpour , M. Soulati Heshajin , A. Kazemzadeh and M. Zakeri, "Synthesis of nano crystalline hydroxyapatite by using precipation technique", Journal of Alloys and Compounds, 430, 330-333 (2007).
22. N. Rameshbabu, K.P. Rao and T.S. Sampat Kumar, "Accelerated microwave processing of nanocrystalline hydroxyapatite", Journal of Material Science, 40, 6319- 6323 (2005).
23. P. Maiti, Y. Prakash, P. Jaya, J. Nanosci. Nanotechnol. 8, 1858 (2008).
24. R. Murugan and S. Ramakrishna, "Effect of zirconia on the formation of calcium phosphate bioceramics under microwave irradiation", Materials Letters, 58, 230-234 (2003).
25. R. Murugan, S. Ramakrishna, "Bioresorbable composites bone paste using polysaccharide based nano hydroxyapatite", Biomaterials 25, 3829 (2004).
26. R. Ramachandra Rao and T. S. Kannan, "Synthesis and sintering of hydroxyapatitezirconia composites", Mater. Sci. Eng., 20, 187 (2002).

27. R.Ramachandra Rao and T. S. Kannan, "Synthesis and sintering of hydroxyapatitezirconia composites", Mater. Sci. Eng., 20, 187 (2002).
28. S. B. Kennedy, N. R. Washburn, C. G. Simon Jr. and E. J. Amis, "Combinatorial screen of the effect of surface energy on fibronectin-mediated osteoblast adhesion, spreading and proliferation", Biomaterials, 27, 3817-3824 (2006).
29. S. J. Kalita, S. Bose, H. L. Hosik and A. Bandyopadhyay, "CaO-P2O5-Na2O based sintering additives for hydroxyapatite (HAp) ceramics", Biomaterials, 25, 2331-2339 (2004).
30. S. Nath, K. Biswas, B. Basu, "Phase stability and microstructure development in hydroxyapatite –mullite system", Scripta Materialia, 58, 1054-1057 (2008).
31. S. Nayar , A. Sinha, "Systematic evolution of a porous hydroxyapatite-poly(vinyl alcohol)-gelatin composite", Colloids and Surfaces B: Biointerfaces, 35, 29-32 (2004).
32. S. Ramesh, C.Y. Tan, I. Sopyan, M. Hamdi and W.D. Teng, "Consolidation of nanocrystalline hydroxyapatite powder", Science and Technology of Advanced Materials, 8, 124-130 (2007).
33. S. Velayudhan, P. Ramesh, H. K. Varma, K. Friedrich, "Dynamic mechanical properties of hydroxyapatite-ethylene vinyl acetate copolymer composites", Materials Chemistry and Physics, 89, 454-460 (2004).
34. S. Velayudhan, P. Ramesh, H. K. Varma, K. Friedrich, "Dynamic mechanical properties of hydroxyapatite-ethylene vinyl acetate copolymer composites", Materials Chemistry and Physics, 89, 454-460 (2004).
35. S.H. Park, I.Y. Ryu, D.J. Kim, J.S. Han and M.H. Lee, "Influence of hydrothermal reaction temperature and ph on phase stability of hydroxyapatite", Key Engineering Materials, 330-332, 147-150 (2007).

36. W. Pyda, A. Slosarczyk, M. Haberko, Z. Paszkiewicz, A. R. Kmita and A. Pyda, "Effect of chemical composition and morphology of zirconia particles on properties of HAP zirconia particulate composites", Key Engineering Materials, 206-213, 1567-1570 (2002).

37. Y. Li and D. li, "Preparation of nano carbonate - substituted hydroxyapatite from an amorphous precursor", International Journal of Applied Ceramic Technology, 5, 442-448 (2008).

38. Z. Yang, Y. Jiang, Y. Wang, L. Ma and F. Li, "Preparation and thermal stability analysis of hydroxyapatite derived from the precipitation process and microwave irradiation method", Materials Letters, 58, 3586-3590 (2004).

39. Z.E. Erkmen, Y. Genc and F. N. Oktar, "Microstructural and mechanical properties of hydroxyapatite –zirconia composites", J. Am. Ceram. Soc, 90, 2885-2892 (2007).